NPS OC-97-008

NAVAL POSTGRADUATE SCHOOL
Monterey, California

THESIS

TEN YEARS OF HYDROGRAPHIC VARIABILITY OFF CENTRAL CALIFORNIA DURING THE UPWELLING SEASON

by

Kenneth A. Baltz

December, 1997

Thesis Advisors:

Curtis A. Collins
Franklin B. Schwing

Approved for public release; distribution is unlimited.

19980427 165

NAVAL POSTGRADUATE SCHOOL

MONTEREY, CALIFORNIA 93943-5000

RADM MARSHA J. EVANS
Superintendent

Released by:

DAVID W. NETZER
Associate Provost and Dean of Research

REPORT DOCUMENTATION PAGE

Form Approved OMB No. 0704-0188

1. AGENCY USE ONLY (Leave blank)	2. REPORT DATE December 1997	3. REPORT TYPE AND DATES COVERED Master's Thesis

4. TITLE AND SUBTITLE	5. FUNDING NUMBERS
Ten Years of Hydrographic Variability off Central California during the Upwelling Season	DW17955338-01-0

6. AUTHOR(S) Kenneth A. Baltz

7. PERFORMING ORGANIZATION NAME(S) AND ADDRESS(ES) Naval Postgraduate School Monterey CA 93943-5000	8. PERFORMING ORGANIZATION REPORT NUMBER

9. SPONSORING/MONITORING AGENCY NAME(S) AND ADDRESS(ES)	10. SPONSORING/MONITORING AGENCY REPORT NUMBER

11. SUPPLEMENTARY NOTES
The views expressed in this thesis are those of the author and do not reflect the official policy or position of the Department of Defense or the U.S. Government.

12a. DISTRIBUTION/AVAILABILITY STATEMENT Approved for public release; distribution is unlimited.	12b. DISTRIBUTION CODE

13. ABSTRACT (maximum 200 words)

Analysis of mean conditions and variability during the upwelling season off central California was performed on data sets of buoy and shoreline surface measurements and CTD data from ten annual NMFS surveys (1987-1996). Climatologies of the surface conditions (alongshore wind, SST, SSS) revealed that the height of the upwelling season occurred during May and June. Variability in the surface conditions was high both inter-annually and inter-seasonally with maximum equatorward wind, lowest SST, and highest SSS during the months of May and June. Ten year climatologies of hydrographic conditions from CTD data (depth and salinity on density anomaly surfaces, and temperature, salinity, density at discrete depths) indicated complex circulation patterns and water mass properties. The nearshore region contained relatively dense, upwelled water and isopycnal gradients conformed to local bathymetry. A robust upwelling filament off Pt. Reyes and three anticyclonic eddy-like features west of the shelf break appeared in the climatologies. EOF (Empirical Orthogonal Function) analysis of the subsurface variability confirmed the presence of the prominent features that appeared in the climatologies. The geophysical signals of the first three EOF-amplitude pairs represent a cross-shore mean upwelling pattern, an alongshore pattern caused by spatial variations in wind and gradients of water mass characteristics, and a filament-eddy resolving pattern, respectively.

14. SUBJECT TERMS Upwelling, Density Surfaces, Eddies, Hydrography, California Current System			15. NUMBER OF PAGES 331
			16. PRICE CODE

17. SECURITY CLASSIFICATION OF REPORT Unclassified	18. SECURITY CLASSIFICATION OF THIS PAGE Unclassified	19. SECURITY CLASSIFICATION OF ABSTRACT Unclassified	20. LIMITATION OF ABSTRACT UL

NSN 7540-01-280-5500

Standard Form 298 (Rev. 2-89)
Prescribed by ANSI Std. 239-18 298-102

TEN YEARS OF HYDROGRAPHIC VARIABILITY OFF CENTRAL CALIFORNIA DURING THE UPWELLING SEASON

Kenneth A. Baltz
Lieutenant, NOAA Corps
B.S., Florida Institute of Technology, 1987

Submitted in partial fulfillment
of the requirements for the degree of

MASTER OF SCIENCE IN PHYSICAL OCEANOGRAPHY

from the

NAVAL POSTGRADUATE SCHOOL
December 1997

Author: _____
Kenneth A. Baltz

Approved by: _____
Curtis A. Collins, Thesis Advisor

_____
Franklin B. Schwing, Co-Advisor

_____
Robert H. Bourke, Chairman
Department of Oceanography

ABSTRACT

Analysis of mean conditions and variability during the upwelling season off central California was performed on data sets of buoy and shoreline surface measurements and CTD data from ten annual NMFS surveys (1987-1996). Climatologies of the surface conditions (alongshore wind, SST, SSS) revealed that the height of the upwelling season occurred during May and June. Variability in the surface conditions was high both inter-annually and inter-seasonally with maximum equatorward wind, lowest SST, and highest SSS during the months of May and June. Ten year climatologies of hydrographic conditions from CTD data (depth and salinity on density anomaly surfaces, and temperature, salinity, density at discrete depths) indicated complex circulation patterns and water mass properties. The nearshore region contained relatively dense, upwelled water and isopycnal gradients conformed to local bathymetry. A robust upwelling filament off Pt. Reyes and three anticyclonic eddy-like features west of the shelf break appeared in the climatologies. EOF (Empirical Orthogonal Function) analysis of the subsurface variability confirmed the presence of the prominent features that appeared in the climatologies. The geophysical signals of the first three EOF-amplitude pairs represent a cross-shore mean upwelling pattern, an alongshore pattern caused by spatial variations in wind and gradients of water mass characteristics, and a filament-eddy resolving pattern, respectively.

TABLE OF CONTENTS

viii

ACKNOWLEDGEMENTS

Many times during this graduate work I felt like I was riding on the shoulders of some very intelligent and hard working people. There are a number for whom I wish to extend my gratitude towards. To my advisors Dr. Franklin Schwing and Dr. Curtis Collins for their guidance, support and fine minds. To the Groundfish Analysis Group of the National Marine Fisheries Service Laboratory at Tiburon, CA; especially Steve, Keith, David, and Dale. To the Officers and Crew of the NOAA Ship David Starr Jordan for their tireless, consistent, professional work in collecting the oceanographic data over the last decade. A special thanks is extended to LCDR John Steger for his tutelage and insightful troubleshooting of my MATLAB code while at the same time making it seem as if I was doing him a favor. He is a superb example of an Officer and a friend. To Dr. George Boehlert, director of Pacific Fisheries Environmental Laboratory, for the support and freedom extended to me to pursue this work and my work at PFEL over the last two years. To all my other colleagues within NOAA who provided valuable input and encouragement during this project. And last but not least to my lovely wife Marie, I wish to extend my sincere appreciation for her continuous loving support and for putting up with the working hours.

I. INTRODUCTION

Ocean water properties and their variability off the central California coast during the upwelling favorable months of May and June are the focus of this paper. From 1987 to 1996, the National Marine Fisheries Service's (NMFS) annual juvenile rockfish survey consistently collected water property data through the use of shipboard Conductivity-Temperature-Depth (CTD) recorders over a thirty to forty day period during May and June. This paper will summarize the annual, interannual, and ten year mean ocean water properties and mesoscale water mass characteristics off central California. The region of study encompasses the upper 200 meters of water from Point Reyes south to Cypress Point and out to approximately eighty kilometers from the shoreline. High temporal resolution wind and sea surface temperature data from environmental data buoys along with sea surface temperature and sea surface salinity from Southeast Farallon Island were analyzed in conjunction with the CTD data. Analysis of water mass characteristics and the spatial-temporal variability of these characteristics is the major impetus of this paper.

Water temperature, salinity, and density at discrete depths produce spatial signatures of specific water masses and circulation patterns as well as complex mixing of water masses. Data from the NMFS surveys show that during the height of the upwelling season, water properties in the study region are distinct from those of the California Current. Strong persistent upwelling favorable winds during the survey periods coupled with the unique geography and bathymetry of central California produce regionally distinct water circulation patterns coupled with mixed water types.

1

The objective of this research is to more fully understand the dynamics of the physical processes at work in the central California coastal region. Understanding the physical processes in this region, will also help in the understanding of the environmental linkages to the fisheries ecosystem which play a significant role in causing variability in species.

II. BACKGROUND

Previous studies have shown that the central California coastal waters are hydrodynamically complex. The California Current (CC) dominates the large-scale, seasonal circulation along California (Hickey, 1979). The CC is the eastern limb of the large scale, anticyclonic gyre of the subtropical North Pacific ocean. Except near the coast, the CC is a relatively broad, complex and energetic current which extends from the surface to 300 meters depth (Hickey, 1996). The CC carries water equatorward throughout the year along the North American west coast to the North Equatorial Current (Lynn and Simpson, 1987). Seasonal differences of water masses and seawater temperatures in the central California region have provided a basis for defining three distinct oceanographic seasons: upwelling, oceanic, and Davidson Current (Breaker and Broenkow, 1994). The start of the highly productive upwelling season off central California is marked by the spring transition, a rapid progression to sustained northwesterly winds along the coast (Huyer et al., 1979; Strub et al., 1987; Lentz, 1987). This transition usually occurs during April but may start as early as March and as late as May (Huyer, 1983; Sakuma et al., 1996). Steepened gradients between the North Pacific high pressure system and a thermal low over the southwestern United States during the upwelling season results in persistent northwesterly winds along the west coast (Halliwell and Allen, 1984). The frictional stress of equatorward wind on the ocean's surface, in concert with the earth's rotation, causes water in the surface layer to move away from the western coast of continental land masses (Sverdrup et al., 1942), such as the California coast. The offshore moving surface water, referred to as Ekman transport after the scientist who

3

first explained this process (Ekman, 1905), is replaced by water which upwells along the coast from depths of 50 to 100 meters or more.

As upwelling favorable conditions commence, coastal sea surface temperature (SST) cools abruptly and coastal sea surface height lowers within the spring transition period; these conditions persist throughout the duration of the upwelling season. Coastal circulation during upwelling season is highly variable and difficult to quantify, and is driven primarily by the local wind field (Parker, 1996). Upwelled water is not only cooler but is more saline than the original surface water (Huyer 1983; Kosro et al., 1991) and typically has much greater concentrations of nutrients that are key to initiating and sustaining biological production (Smith, 1968; Traganza et al., 1981; Kosro et al., 1991). This is why marine ecosystems in eastern boundary currents that are associated with coastal upwelling are highly productive, and capable of maintaining large standing crops of plankton, massive fish stocks such as sardines and anchovies, and major populations of marine mammals and sea birds (Ryther 1969; Walsh et al., 1977; Wroblewski, 1977). Although the major eastern boundary currents comprise only a small percentage of the total global ocean, they are responsible for 40% of the world's fish harvest (Botsford, 1997). The world's major eastern boundary currents that are associated with significant coastal upwelling include the Canary off the Iberian peninsula and northwestern Africa, the Peru (or Humboldt) off western South America, the Leeuwin off western Australia, and the California Current System off western North America (Schwing et al., 1997).

Analysis of the extensive California Cooperative Oceanic Fisheries Investigations (CalCOFI) data record has consistently shown that the largest and most complex changes in

circulation and water mass interactions occur in the coastal region of Central California north of 34°N, and are associated with seasonal upwelling (Lynn, 1967; Lynn and Simpson, 1987). CalCOFI data from the 1940s, 50s and 60s provided the earliest evidence of the seasonal variation of water mass characteristics and large scale current patterns in the CC system. The water properties of the CC system are determined by four water masses, each defined by its temperature, salinity, dissolved oxygen, and nutrients. Pacific Subarctic water forms at high latitudes in regions of excess precipitation and heat loss. This water is entrained in the Subarctic Current and West Wind Drift, and it enters the CC near 48°N. It has relatively low temperature, low salinity, high dissolved oxygen and high phosphate. Water of Pacific Subarctic origin is still recognizable by its relatively low salinity in the core of the CC near 25°N. Pacific Subarctic water gives the CC its offshore near-surface salinity minimum and high dissolved oxygen concentration. Eastern North Pacific Central water is warm, relatively salty, and low in dissolved oxygen and nutrients. It enters the CC system from the west. Equatorial Pacific water forms in the eastern tropical Pacific and has relatively high temperature, high salinity, high nutrients, and low dissolved oxygen. It enters the deeper-lying California Undercurrent from the south. Upwelling near the California coast brings relatively cold, salty, nutrient rich, and oxygen-deficient water from depth to the surface where it is further modified by air-sea interaction (Sverdrup et al., 1942; Reid et al., 1958; Pickard, 1964).

Lynn (1967) described the seasonal variations of temperature and salinity at 10 meters in the CC based on CalCOFI data. His resulting charts show 13 year mean isopleths of temperature and salinity off the central California coast near the San Francisco Bay are

oriented parallel to the coast with temperature(salinity) minima(maxima) occurring near Pt. Reyes. Temperature(salinity) increases(decreases) offshore and southward from Pt. Reyes to Pt. Conception. The chart of standard deviations for salinity shows a coastal maximum in the vicinity of San Francisco Bay. This same region shows the largest mean seasonal salinity range. Lynn's harmonic analysis of the CalCOFI data indicates that in the upwelling regions along central California, the maximum salinity is in the summer, shortly after the minimum temperatures occur.

Lynn and Simpson (1987) examined the seasonal variation of the physical characteristics and large-scale current patterns of the CC system by using harmonic analysis applied to the 1950-1978 CalCOFI data set. Their significant findings in regards to the central California coast are as follows: 1) There are three physical oceanographic domains; oceanic, coastal, and an intervening transition zone, defined by the amplitude and phasing of the seasonal variation of the dynamic height and by the standard deviation of the overall record of dynamic height. In the coastal domain the dynamic height is controlled by alterations in the inshore surface and subsurface current structure. 2) Off central California the CC is near surface. The region of low salinity, high geostrophic velocity core 300-400 km offshore also corresponds to the eddy-dominated transition zone. 3) Off central California the core of the equatorward flowing CC moves closest to shore during May with only a vestige of the poleward flowing California Undercurrent. The strongest inshore equatorward flow of the CC occurs in April-May. 4) Distribution of water characteristics shows that there is a strong interaction between the core of the CC and the mesoscale eddy field. 5) Below the surface layer (or upper thermocline) the seasonal variation of water mass characteristics is

related to both the vertical adjustment of the water column to seasonally varying geostrophic currents and to varying transport of waters from different sources.

The Coastal Transition Zone (CTZ) program, a multi-disciplinary survey performed in 1987 and 1988, made progress in resolving the dynamics of the interactions between the California Current and coastal waters during the upwelling season off the northern California coast (Brink and Cowles, 1991). After the spring transition, persistent equatorward wind stress establishes an upwelling state along the coast. As coastal waters are advected offshore, cooler, more saline water is vertically advected to replace it, setting up an offshore increase in sea surface slope (Kosro et al., 1991). Persistent upwelling-favorable conditions cause the thin band of recently upwelled water to widen along the coast. This band is separate from warmer, fresher offshore water by a frontal zone, whose gradients of temperature and salinity vary in steepness spatially and temporally (Kosro et al., 1991). Along this frontal zone, it is thought that an alongshore baroclinic current, or jet, develops and meanders on and offshore (Ramp et al., 1991). Brink et al. (1991) shows that long-term drifter data indicates that meanders of an alongshore baroclinic jet expand in the cross-shore direction with decreasing latitude. In general, the results from the CTZ program reveal that the core of the CC in summertime is unstable, leading to the formation of a meandering jet surrounded by persistent eddies. Eddies on the order of 100 km diameter that develop inshore of this jet are thought to entrain cold upwelled water and advect it seaward in the form of filaments. These filaments extend up to 250-300 km offshore, penetrating past 200 m depth and have a lifespan of about one month (Ramp et al., 1991).

Smaller scale physical oceanographic data analysis in the central California coastal

7

region identified upwelling and upwelling relaxation states as distinct circulation and water property regimes, with rapid transition periods between the two. Send et al.'s (1987) model of relaxation is based on data from current moorings on the shelf north of Point Reyes (The Coastal Ocean Dynamics Experiment - CODE) which showed a strong correlation between wind relaxation, increased poleward flow, and increased temperature. They concluded that during relaxation, cross-shore advection was small and northward alongshore advection of solar-heated waters was responsible for a rise in temperatures. Rosenfeld et al. (1994) focused on Monterey Bay, where three persistent features were found during the upwelling season. First was the presence of warm and salty water inside the northern bight of Monterey Bay southeast of Santa Cruz. Described in Graham et al. (1992) as an "upwelling shadow", this region is considered to be in the lee of upwelling favorable winds. A relatively longer residence time due to weak vertical wind mixing combined with increased surface heating, is thought to cause near surface waters in the bight to have a warmer signal than nearby cold upwelled water. The second feature found during the upwelling season was an equatorward filament advecting cold water upwelled at the Pt. Año Nuevo upwelling center across the mouth of Monterey Bay. Upwelling centers along this region of the coast are usually located near a coastal point or cape. Satellite imagery correlated with hydrographic measurements revealed the Pt. Año Nuevo filament extending equatorward during persistent upwelling conditions. During episodic relaxation from upwelling, circulation and water properties respond quickly to the change in wind forcing, displaying characteristics unique to relaxations. The third upwelling feature observed was the development of a warm, fresh anticyclonic eddy at the mouth of Monterey Bay upon the return of upwelling that immediately followed a

relaxation event. Another significant finding by these and other investigations of coastal upwelling dynamics is the tendency for oceanic surface waters, which have been pushed offshore by Ekman transport, to collapse coastward almost immediately upon relaxation of the alongshore wind (Roughgarden et al., 1991; Smith, 1994). The wind only has to relax substantially from a higher intensity that had been maintained over some previous period. It is almost as if the system were "spring-loaded", building up tension by the pushing of surface waters offshore and then suddenly springing back when tension is released (Bakun, 1996).

Breaker and Mooers (1986) found that mesoscale variability of ocean conditions off the central California coast is strongly influenced by coastal upwelling and related processes. Their study off the Big Sur coast (Monterey Bay to Pt. Piedras Blancas) concludes that there is significant space-time variability in ocean properties over periods of days and distances of several tens of kilometers. The internal density field, averaged over space (120 km alongshore) and time (18 days), reveals characteristics of a coastal upwelling regime, including an equatorward surface jet 25 km to 40 km offshore and weaker poleward flow below 150m and within 20 km of the coast. Upper ocean circulation is strongly influenced by the bathymetry offshore to water depths of at least 100m. Specifically during spring and summer, movement of a coastal upwelling front, often located between 15 km and 50 km offshore is a major contributor to cross-shore variability. The upwelling front meanders with an alongshore scale of about 80 km, and a time scale of 30 to 40 days. The alongshore mean position of the major upwelling front migrates offshore during spring and summer. Offshore displacement of the front may be caused by Ekman transport over periods of days-to-weeks, and by Rossby wave dispersion over longer periods. During summer the Breaker and Mooers

9

study found that a time-dependent offshore scale based on Rossby wave dynamics was more appropriate than the baroclinic Rossby radius.

Schwing et al. (1991) examined hydrographic data collected from south of Monterey Bay to north of Pt Reyes in May-June 1989 and found that equatorward currents were predominant in the upper 200m, upon which numerous eddy-like features were superimposed. Upwelling favorable winds strengthened and relaxed at 3-10 day intervals, and upwelling was centered north of Pt. Reyes, near Pt. Año Nuevo, and at Pt. Sur, producing alongshore and cross-shelf fronts.

Analysis of SST from offshore buoys within the same region off the central California coast along with observations of meteorological variables shows that the central California coast is the site of the strongest and most persistent wind forcing along the U.S. west coast (Dorman and Winant, 1995). The central California coastal mountain range usually extends above the marine boundary layer and serves to steer the wind in a direction parallel to the coast. The strong winds aligned with the coast provide the motive force behind the upwelling processes during the spring and summer. This, in turn, explains the different phases of the annual temperature cycle; minimum temperatures are observed in spring, at the height of the upwelling, due to vertical advection of colder water. The air temperature tracks the water temperature in this cycle, reaching minimum values during the spring also.

The well traversed, yet little studied Gulf of the Farallones is a unique region of the central California coastal area due to its proximity to the outflow of San Francisco Bay, Pt. Reyes and the Farallon Islands along with its unique bathymetry in regards to the continental shelf. The Gulf of the Farallones occupies a significant portion of the region that is the focus

of this thesis. Analysis of the seasonal variability in circulation and water masses during 1991 and 1992 within the Gulf of the Farallones by Steger (1997, in press) reveals much complexity in the physical oceanographic dynamics. Biharmonic fits to daily winds measured at a buoy within the Gulf of the Farallones show an annual pattern of weak winds in December-February and strong equatorward winds in April-June. Winds from the harmonic analysis of multiple buoy data in the Gulf are weaker than those measured north of the Gulf (off Bodega Bay) and south of the Gulf (off Half Moon Bay), possibly due to the partial lee created by Pt. Reyes. Week-to-week variability is as great as the season-to-season or interannual changes. Harmonic analysis of daily buoy sea surface temperature follow an annual pattern, but unlike the wind the seasonal sea temperature cycles are characterized by two maxima/minima. After seasonal warming in late winter, temperatures again decline due to coastal upwelling, reaching a minimum in mid-May. Sea temperatures at the buoy inside the Gulf are less affected by spring winds than adjacent buoy temperatures outside the Gulf.

The annual cycle of subsurface hydrography is described by Steger through characterizing the water over the continental slope between 50-200m depth. Beginning in February temperatures vary from 8-11°C and salinities vary from 33.4-34.0 ppt. Isopycnals are nearly horizontal, suggesting geostrophic currents are weak. By May, the strong upwelling favorable winds of the season have produced a marked oceanic response. The Gulf becomes filled with cooler and saltier water. Isopycnals are tilted upwards towards the coast, suggesting geostrophic currents may be carrying some of the cooler, saltier water from the north. By August temperatures and salinities have returned to those seen in February. Isopycnals are sloped steeply downwards towards the coast, suggesting that poleward

11

geostrophic currents carrying warmer water northward. In the upper 50m, there is more horizontal variability in the hydrography. Except for San Francisco Bay outflow, warmer and fresher waters are always offshore of the Gulf. Near-surface waters in February 1991 are ~12°C; cool in May to ~9.5°C; then warm in August to ~15°C with late summer solar heating and lighter winds; and cool during the fall weather to ~13°C by the end of October. Near-surface salinities remain 33.3-33.4 ppt except during the May upwelling season when from 33.2-33.9 ppt are found.

The flow regime in the Gulf during May is quite different from that during the winter and fall. There is no equatorward jet off Pt. Reyes, but hydrography shows that cool, saline water stretches across the shelf off Pt. Reyes and southward. Near the Farallon Islands, the pool of cool, saline water extends two tongues, one southeastward along the coast and a second southwestward. As the western tongue moves offshore it accelerates. Warm, fresher water impinges on the slope of the Gulf from both north and south. The flow is much more baroclinic in May than in the winter. The flow over the slope at 100m depth is generally poleward though weak and meandering. The offshore flow is still fairly strong but the equatorward jet in the north is barely evident. The upwelling favorable conditions during May have a significant effect on water mass characteristics of the upper water layers and even down to 200m depth with the result being cooler and saltier water than in the winter months. Residence times for water in the entire Gulf is calculated to be ~6 days during May 1991. Waters over the shelf have a slightly higher residence time (6.4 days) and the water over the slope have a slightly shorter residence time (5.0 days).

The oceanographic community has come to realize that a major influence on the

physics and biology of California's coastal ocean is the occasional occurrence of events called El Niño or ENSO (El Niño-Southern Oscillation). On California's coast, ENSOs are manifested as 1 or 2 year periods with warmer temperatures, higher sea levels, a weaker equatorward CC and lower biological productivity. Every four to five years, during 1971-1984, ENSO episodes produced warmer coastal sea surface temperatures off central California. Most of the warming occurred during fall and winter. ENSO episodes were often followed by major spring transitions (Breaker and Mooers, 1986).

Another important recent finding is that ocean conditions also vary on several spatial scales, over longer time scales than interannual variability or the 4 to 10 year variability of ENSO events. In central California coastal regions as well as other locations in the North Pacific, atmospheric and ocean conditions, plus the associated marine ecosystems, appear to change in a fundamental way every 30 to 60 years. Such changes from one oceanographic regime to another are known as regime shifts. A good example of this is the dramatic shift in a number of atmospheric and oceanographic variables in the eastern North Pacific coincident with intensification of the Aleutian low pressure system in the mid-1970s (Botsford, 1996).

The National Oceanic and Atmospheric Administration (NOAA) NMFS Tiburon Laboratory juvenile rockfish surveys have been conducted annually during the May-June period. Since 1987 these surveys have collected physical oceanographic data at consistent coastal and offshore stations in the area bounded by Pt Reyes (38.17°N) to the north and Cypress Pt. (36.58°N) to the south, extending approximately 80 km offshore (Sakuma et al., 1996). This region is characterized by several important dynamic processes and features that

13

contribute to a complex circulation (Schwing et al., 1991). Significant physical processes taking place during the periods of the juvenile rockfish surveys include wind forced motions (e.g., upwelling, horizontal advection, vertical mixing), tides, buoyancy effects (e.g., heat exchange with the atmosphere, freshwater inflow), and the large scale California Current system. High resolution satellite imagery of sea surface temperatures in this region during the height of the upwelling season is striking in its complexity (Figure 1) and clearly identifies several prominent coastal points that are sites of preferred upwelling (e.g., Pt. Reyes, Pt. Año Nuevo, and Pt. Sur) (Schwing et al., 1991, Rosenfeld et al., 1994).

Water masses of unique characteristics may enter the survey region via local upwelling, advection onshelf or alongshelf due to changes in wind stress, and freshwater discharge, primarily from San Francisco Bay. Solar insolation on surface waters in shallow shelf regions also adds a measurable contribution to water characteristics in this region. The rich complexity of the coastal topography of the central California coast distinguishes it from other sections of coastline along North America (Dorman and Winant, 1995). Bathymetry in this region is diverse, and includes features on a range of scales that could profoundly influence the circulation throughout the survey region. These features include submarine canyons (e.g., Monterey Canyon, Pioneer Canyon, Carmel Canyon), banks, seamounts, headlands and embayments of various dimensions, and a wide range of continental shelf and slope widths (Figure 2). The NMFS survey region is inshore of the coastal transition zone described by CTZ collaborators, south of the CODE study area, and north of the Pt. Sur study area (Ramp et al., 1997; Collins et al., 1996; Tisch et al., 1992; Ramp and Abbott, 1992; Breaker and Mooers, 1986). The dynamics of water mass mixing, flow patterns and

14

upwelling circulation in this survey region are distinct, and represent a complex combination of the characteristics described to the north, south, and west.

The 10 year (1987-1996) time series of physical oceanographic data from the NMFS study provides insight into the mean mesoscale flow patterns, water masses, and spatial/temporal variability of the significant physical oceanographic parameters. Analysis of the region's four NOAA environmental data buoys' measurements along with the analysis of the long time series of daily recordings of sea surface temperature and sea surface salinity at Southeast Farallon Island helps to describe the timing and strength of the important seasonal wind forcing, quantifies the annual/seasonal temperature and salinity signal, and provides insight to the variability of these physical variables. The objective of this thesis is to describe the climatological, interannual and seasonal conditions of water masses found off and along central California during the upwelling season along with the implied flow patterns of these waters and the spatial-temporal variability over the ten year study period. Understanding the physical processes occurring in this region will help to better determine the environmental linkages which play a part in controlling variability of the natural resource ecosystem.
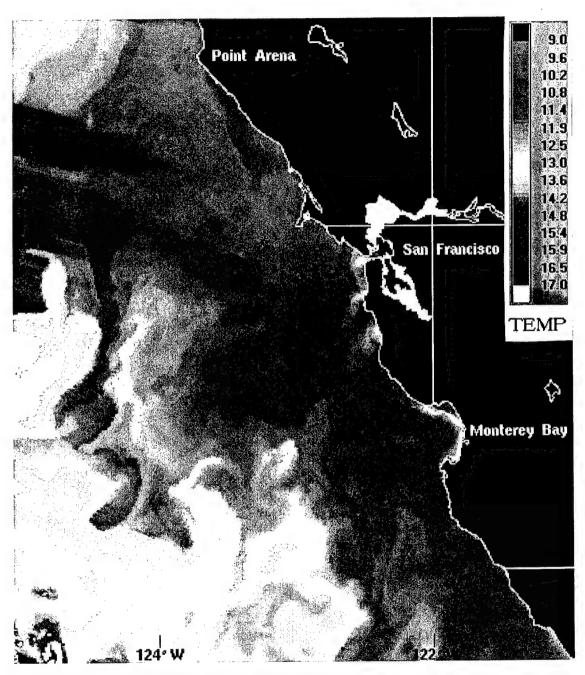
Figure 1. AVHRR Satellite Image of Sea Surface Temperature off Central California,

June 10, 1996, Image Resolution is 1.1 km, Temperature Scale is in Degrees Celsius

3-Dimensional View of the Bathymetry of the NOAA NMFS Survey Region

Figure 2

III. DATA AND METHODS

A. CRUISE DESIGN

The results of annual cruises during May and June of each year from 1987 to 1996 are studied in this thesis. These cruises are the young-of-the-year (YOY) rockfish surveys conducted by the NOAA, National Marine Fisheries Service, Tiburon Laboratory aboard the *NOAA Ship David Starr Jordan* (DSJ). The survey station grid remained consistent from year to year and included the area bounded by Cypress Point (36.58°N) to the south and Pt. Reyes (38.17°N) to the north, and thence from the coastline to approximately 80 km offshore. Figure 3 displays the location of the survey stations, the bathymetry of the region, and the location of the four NOAA weather buoys within the survey region.

The data collection routine at standard sampling stations consisted of nighttime midwater trawls, set consecutively at 30m depth for 15 minutes, immediately followed by Conductivity-Temperature-Depth (CTD) casts. Daytime operations focused on casts at standard CTD sampling stations (Figure 4). Prior to 1992, CTD casts were usually deployed to 200 meters depth or within 10m of the bottom at stations shallower than 200 meters. After 1991 CTD casts were deployed to a maximum depth 500 meters whenever possible. Three consecutive "sweeps" (or repeated sampling) of the station grid was performed from south to north over a period of roughly 10 days during each annual cruise. The dates for each annual May-June cruise and for all "sweeps" are listed in Table 1. A more complete description of cruise operations and CTD data collection is given by Sakuma et al. (1996).

19

CTD Stations and Buoy Positions During May/June Cruises

open circle – CTD

cross within circle – Trawl & CTD

B – NOAA Buoy
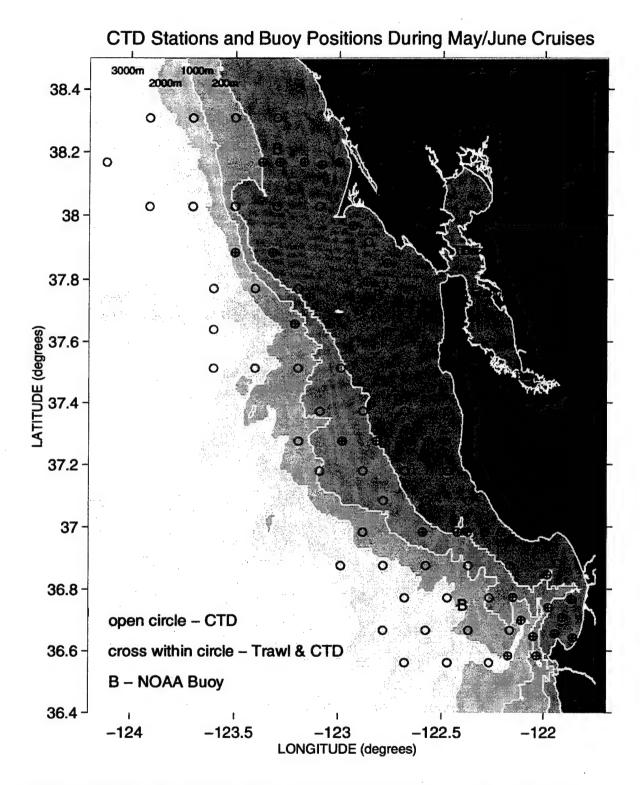
Figure 3. Stations were sampled 3 times during each annual survey cruise (1987-1996).

20

Table 1. Cruise and sweep dates during the 1987-1996 NMFS YOY rockfish surveys

YEAR	CRUISE-SWEEP	DATES
1987	DSJ8705-1	MAY 23 - MAY 29
1987	DSJ8705-2	MAY 30 - JUNE 07
1987	DSJ8705-3	JUNE 12 - JUNE 20
1988	DSJ8806-1	MAY 22 - JUNE 01
1988	DSJ8806-2	JUNE 02 - JUNE 11
1988	DSJ8806-3	JUNE 11 - JUNE 18
1989	DSJ8904-1	MAY 14 - MAY 22
1989	DSJ8904-2	MAY 22 - JUNE 03
1989	DSJ8904-3	JUNE 04 - JUNE 13
1990	DSJ9005-1	MAY 13 - MAY 21
1990	DSJ9005-2	MAY 22 - MAY 30
1990	DSJ9005-3	JUNE 01 - JUNE 10
1991	DSJ9105-1	MAY 14 - MAY 22
1991	DSJ9105-2	MAY 27 - JUNE 03
1991	DSJ9105-3	JUNE 03 - JUNE 10
1992	DSJ9206-1	MAY 11 - MAY 18
1992	DSJ9206-2	MAY 18 - MAY 26
1992	DSJ9206-3	JUNE 04 - JUNE 16
1993	DSJ9307-1	MAY 13 - MAY 20
1993	DSJ9307-2	MAY 21 - MAY 28
1993	DSJ9307-3	JUNE 03 - JUNE 10
1994	DSJ9406-1	MAY 18 - MAY 25
1994	DSJ9406-2	MAY 26 - JUNE 02
1994	DSJ9406-3	JUNE 11 - JUNE 18
1995	DSJ9506-1	MAY 17 - MAY 26
1995	DSJ9506-2	MAY 27 - JUNE 03
1995	DSJ9506-3	JUNE 08 - JUNE 15
1996	DSJ9606-1	MAY 18 - MAY 25
1996	DSJ9606-2	MAY 26 - JUNE 02
1996	DSJ9606-3	JUNE 10 - JUNE 19

B. CTD DATA COLLECTION AND PROCESSING

CTD data were collected using a Sea-Bird Electronics, Inc., SEACAT-SBE-19 profilers while underway aboard the *NOAA Ship David Starr Jordan* during the annual NMFS juvenile rockfish surveys. During deployment, the vessel was hove to and the profiler was attached to a hydrographic winch cable. The profiler was suspended just beneath the surface for two minutes to allow the conductivity and temperature sensors to equilibrate. An average descent rate of 45 meters/minute was then used to lower the instrument. Only data collected on the downcasts were used for analysis. All data were merged and averaged into equally spaced 2 meter depth bins. Each depth bin contains position information (latitude and longitude), date, depth, temperature , salinity, and potential density anomaly (σ_θ).

Two-meter hydrographic data were used to construct temperature versus salinity diagrams for each year as well as a ten year mean TS diagram. The TS diagrams show the temperature, salinity, and density at discrete depths from 10 to 500 meters. Horizontal charts of selected CTD variables were produced for all 30 sweeps that occurred from 1987-1996.

Spatial grids of the sampling region were created for contour plotting of the selected CTD variables. Grid point values of the CTD variables were determined by finding all data within a 10 nautical mile radial distance of the grid point and calculating a distance-weighted average. The inverse of the distance squared was used as the distance weighting function. Grid points were equally spaced by 1/6 degree of latitude and longitude (approximately 10 nm). Contoured charts of the selected variables for 10 year climatologies (mean spatial conditions)and their standard deviations were also produced. These variables are depth of the 25.8 kg/m^3 and 26.2 kg/m^3 potential density anomaly surfaces (hereafter referred to as

22

isopycnals), salinity on the 25.8 kg/m³ and 26.2 kg/m³ isopycnals, and the mixed layer depth (MLD).

The 25.8 kg/m³ and 26.2 kg/m³ isopycnals were chosen because they consistently occupied the upper 100 meters of water depth. Depth and salinity on these two isopycnals serve to describe for the dynamics (depth) and water mass characteristics (salinity) both above (25.8 kg/m³ isopycnal) and within (26.2 kg/m³ isopycnal) the halocline. In addition, examining the lateral distribution of subsurface water properties with the use of isopycnal rather than isobaric surfaces eliminates noise due to the vertical excursions of internal waves and internal tides.

Charts of the MLD were produced to better assess the surface layer mixing due to wind stress over. The MLD was determined by using the same criteria adopted by NOAA's National Oceanographic Data Center for determining the MLD at mid-latitudes (Levitus and Monterey, 1997). The MLD is based on a fixed temperature difference $\Delta t = 0.5°C$, where Δt is the temperature difference in degrees Celsius between the ocean surface and the bottom of the mixed layer. This mixed layer depth is considered the water depth at the bottom of the mixed layer. Ten year climatologies of temperature, salinity, and potential density anomaly at 30 meters depth are also presented in order to highlight surface layer water mass characteristics.

Empirical Orthogonal Functions (EOFs) were utilized to determine patterns of temporal and spatial variability on the 25.8 kg/m³ and 26.2 kg/m³ isopycnals. The use of EOF analysis to determine patterns of variance is also known as Principal Component Analysis.

23

EOF analysis, as conventionally applied to oceanographic data sets, is used to decompose space-time distributed data into modes ranked by their variance. The modes or EOFs can be defined as those patterns which are most powerful in explaining the variance of a data set (von Storch and Navarra, 1995). Generally speaking, each mode or EOF has an associated percent of the total variance, a dimensional spatial pattern function, and a dimensionless time series amplitude function. One nice feature of EOF analysis is that it does not require the data to be evenly spaced in time, thus we can analyze the data from May and June to investigate the variability during that period. Scientific investigators should be cautious on two points regarding EOF analysis. First, the solution is indeterminate and therefore an infinite number of solutions exist. Second, the patterns that are generated are open to interpretation. If the patterns make no physical sense, they must be rejected.

For the EOF analysis, four variables, the depth of 25.8 kg/m^3 and 26.2 kg/m isopycnals and salinity on these two isopycnals are placed into space(s)-time(t) distributed data sets $D(s,t)$, where s is the number of spatially distributed grid points, and t is the number of observations over time. t is either 30, the number of sweeps that took place over the years 1987-1996, or 10, the number of years in cases of annual-averaged fields. The spatially distributed grid points are separated by approximately 10 nautical miles (1/6 degree of latitude and longitude). The EOF analysis model can be written

$$D(s,t) = \sum_{k=1}^{K} a_k(t)e_k(s) + \zeta(s,t)$$

24

K is the number of spatial grid points having data for each sweep over the ten years. The EOF analysis decomposes the data set $D(s,t)$ into 3 matrices. The first matrix (a_k) contains the nonzero EOF modes and their associated modal amplitudes. The modal amplitudes can be thought of as temporal variance coefficients for each EOF. This matrix has NxE rows and columns, with N being 30 (sweeps) and E being the number of nonzero EOF modes. The second matrix (e_k) contains the Zscores or spatial pattern eigenvectors with the same size (MxN) as the original data set $D(s,t)$. The third matrix contains the percentage of total variance explained by each of the EOF modes or Principal Components. This matrix has the size $Ex1$. $\zeta(s,t)$ is the residual noise term. Charts of the variance patterns contained in the Zscores of the first three EOF modes are presented along with the total variance explained by the particular EOF mode. Time series plots of the EOF modal amplitudes are also presented.

C.   BUOY DATA COLLECTION AND PROCESSING

Wind and sea temperature data were obtained from 4 NOAA moored environmental data buoys located within the survey area. These four buoys are offshore of Bodega, CA (BUOY# 46013, 38.2°N - 123.3°W), in the Gulf of the Farallones (BUOY# 46026, 37.7°N - 122.8°W), offshore of Half Moon Bay (BUOY# 46012, 37.4°N - 122.7°W), and just west of Monterey Bay (BUOY# 46042, 36.7°N - 122.4°W). The hourly data (mean values from 6 minute recordings) were acquired from data archives at the NOAA National Climatic Data Center. Daily mean values for surface water temperature, along with the eastward and northward components of wind were calculated from the hourly data.

Climatology and variance were determined for SST and alongshore wind at each of

the four buoys by a least squares regression of the daily mean data to an annual and semiannual harmonic signal. The biharmonic analysis is similar to that used by Schwing et al. (1996). The axis for the alongshore wind component (V_r) was determined by calculating the angle of the dominant alongshore direction of the daily mean wind vectors in compass degrees. This was accomplished by a principal component analysis (PCA) of the northward wind component over the entire set of wind data for each of the four buoys. This wind direction or angle can be thought of as the axis that maximizes the alongshore variance dominant and is used as the vertical axis upon which the velocities of the V_r wind are calculated and plotted.

All the archived data from each buoy over the buoy's entire operating period was used in a biharmonic analysis to determine climatology and variance. The buoys' operating periods were: BUOY# 46013 - 1981 through 1996; BUOY# 46026 - 1982 through 1996; BUOY# 46012 - 1980 through 1996; BUOY# 46042 - 1987 through 1996. The biharmonic equation can be written

$$B(t) = A_0 + A_1 cos(2t) + B_1 sin(2t) + A_2 cos(4t) + B_2 sin(4t)$$

where B is the buoy SST or the alongshore component of wind data, t is the year day divided by the number of days in the year (365) and the A_i and B_i terms are coefficients determined by the regression at each buoy. The fits were not significantly improved by including higher harmonics. Standard errors were calculated for each year day, then fit with the same biharmonic model. Climatologies of SST and alongshore wind are presented along with plots of daily SST and alongshore wind during the first six months of each year from 1987-1996.

26

D. FARALLON ISLAND DATA COLLECTION AND PROCESSING

Southeast Farallon Island (SEFI) is situated on the outer part of the continental shelf, near the continental shelf break and at the westernmost region of the Gulf of the Farallones. Since 1926 scientists and volunteers working at SEFI have measured daily SST and collected surface seawater samples for determining salinity. The resulting daily SST and sea surface salinity (SSS) data are archived at Scripps Institution of Oceanography (SIO) as part of their Shore Station Data Program. After the data were acquired from SIO, a biharmonic analysis was used to determine the climatology for SST and SSS. All the data collected since 1926 were utilized in the biharmonic analysis. Using the same technique was as that described in Section B. Climatologies of SST and SSS are presented along with plots of daily SST and SSS during the first six months of each year from 1987-1996.

E. PROGRAMS AND HARDWARE

All statistical analysis and subsequent plotting were accomplished through the use of MATLAB (Matrix Laboratory) version 4.2 and version 5.0 for Unix based operating system, which were run on Silicon Graphics Incorporated (SGI) Indy Workstation computers. MATLAB (version 5.0) along with the MATLAB Statistics Toolbox (version 2.0) *princomp.m* function was used for the Empirical Orthogonal Function (EOF) analysis. MATLAB (version 4.2) along with customized MATLAB code *.m* files were used for all the other data manipulation and analysis. All charts and figures were produced with MATLAB (version 4.2) customized code *.m* files.

IV. RESULTS

A. CLIMATOLOGIES

Climatologies of selected oceanographic variables during May and June are first presented. These define the average conditions and the range of variability in the survey region during the upwelling season.

The alongshore wind and SST climatologies from the buoy data are presented in Figures 4 and 5. In general, the four buoys display similar patterns of daily mean alongshore wind (Figure 4). The bold black curves denote the biharmonic fits to the daily mean data for the buoys' entire period of operation. The light gray shaded area around the biharmonic curves denote plus and minus one standard error, calculated for each year day from the observations on that day, then smoothed with the biharmonic fit. Negative wind velocities indicate equatorward wind. The vertical axis is based on the principal component analysis (PCA) direction, which varies at each buoy due to the adjacent local coastline steering the wind (Dorman and Winant, 1995). The dark gray shaded area denotes the typical survey period. There is a high positive correlation in equatorward wind strength and phasing throughout the survey region. Figure 4 shows that maximum equatorward winds occur during May and June at all four buoys. The persistence of equatorward wind is quite evident throughout the summer and fall months. Mean equatorward wind velocities during the survey period are greatest at buoy 46013 off Bodega, CA, and the two northern buoys (46013 and 46026) have larger mean velocities than the two southern buoys (46012 and 46042).
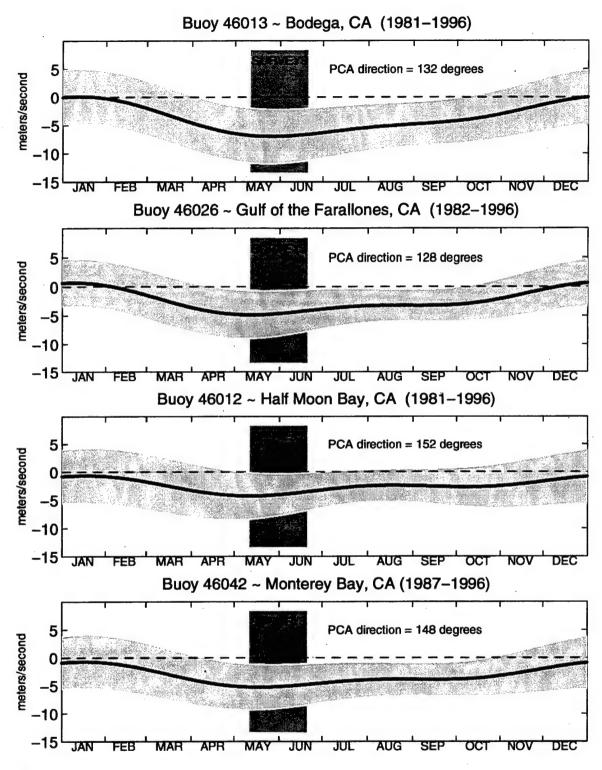
Figure 4. Alongshore wind climatologies from NOAA Buoys. The bold curve denotes the harmonic fits to the daily data. The light gray shaded area around the bold curve is plus and minus one standard error. The dark gray shaded area denotes the survey period.

Highly coherent seasonal signals are apparent in the climatologies of daily SST at all four buoys (Figure 5). Lowest daily mean temperatures are reached during May and June for all buoys when cooler water is upwelled at the coast. Buoy 46013, off Bodega, CA attains the coldest daily mean SSTs (10° Celsius) and has the most obvious "dip" in SSTs during the upwelling season. Mean SSTs are always cooler at the two northern buoys of the survey area. Buoy 46026 (Gulf of the Farallones) has its lowest mean SSTs near 11° C, whereas the lowest mean SSTs at the two southern buoys are near 12° C. The two northern buoys also have larger standard error envelopes for SST than the two southern buoys.

Climatologies of SST and SSS at Southeast Farallon Island (SEFI) illustrate a distinct low SST and high SSS upwelling signal during May and June cruise period (Figure 6). The climatological SST signal mimics that of the Gulf of the Farallones buoy. Annually, the lowest SST and highest SSS occur during May and June at Southeast Farallon Island. The standard error envelope around the biharmonic curve for SSS indicates the high variability during the rainy season which occurs from November to March. With its proximity to the Golden Gate, Southeast Farallon Island and the Gulf of the Farallones SSS is sensitive to the outflowing freshwater lens from the San Francisco Bay during the winter months. The width of the standard error envelope for salinity shrinks continually during the NMFS survey period and into the fall months with minimum standard errors during late September and early October.
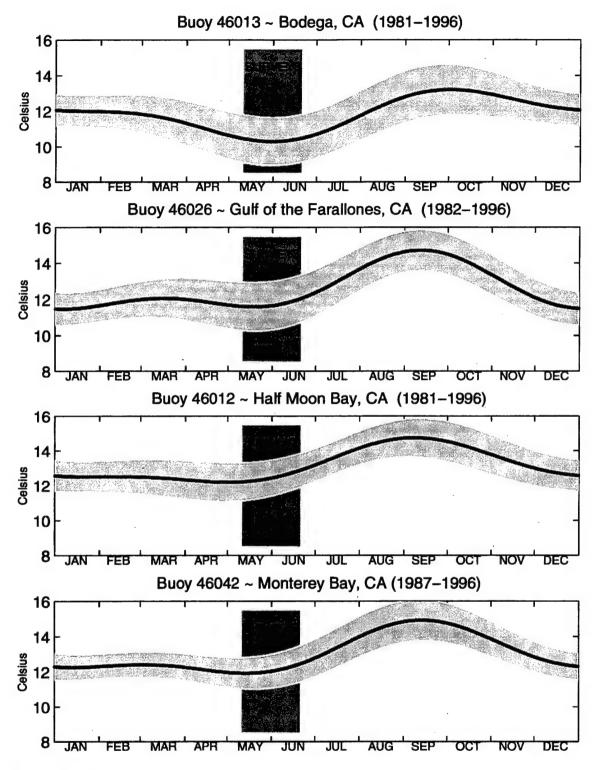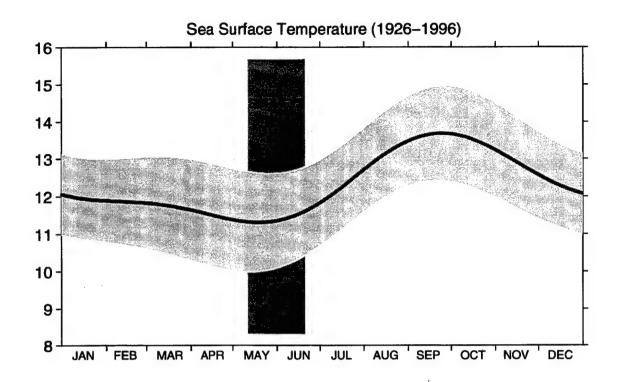
Figure 5. SST climatologies from NOAA Buoys. The bold curve denotes the harmonic fits to the daily data. The light gray shaded area around the bold curve is plus and minus one standard error. The dark gray shaded area denotes the survey period.

Sea Surface Temperature (1926–1996)

Sea Surface Salinity (1926–1996)
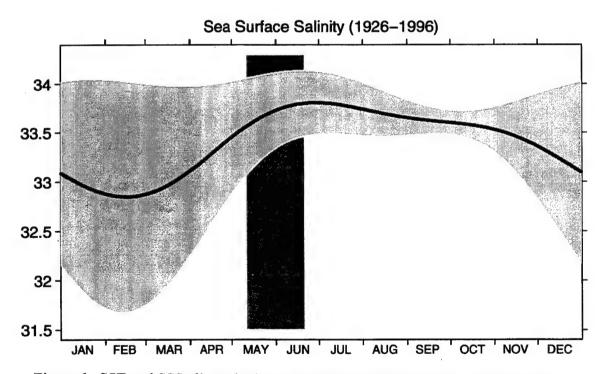
Figure 6. SST and SSS climatologies at Southeast Farallon Island. The bold curve denotes the fits to the daily data. The light gray shaded area around the bold curve is plus and minus one standard error. The dark gray shaded area is the survey period.

The 10 year mean conditions (hereafter referred to as climatologies) of CTD variables from the survey cruise sampling from 1987 to 1996 are presented. The climatologies illustrate the relationship between temperature and salinity at discrete depths from 10 meters to 500 meters (Figure 7). Two years, 1988 and 1992, which displayed the largest contrasts are plotted along with the climatology on a temperature-salinity diagram. 1988 is characterized as cold and salty at all discrete depths between 10 and 200 meters, whereas 1992 is characterized as warm and fresh. On isopycnal surfaces, however, 1988 was relatively warm and saline and 1992, cool and fresh. The TS diagram background of curved density surfaces (isopycnals) illustrates the non-linear relationship between temperature, salinity, water depth, and density. Based on the climatology, the 25.8 kg/m^3 isopycnal occupied the upper water layers near 30 meters depth (range 20-80 m) and the 26.2 kg/m^3 isopycnal occupied deeper waters within the halocline near the 100 meter depth (range of 50-150 m).

Implied circulation patterns and dynamics of the internal density fields in the upper water column can be determined by examining the depth of potential density isopycnals. Horizontal contour charts for climatologies of the 25.8 kg/m^3 and 26.2 kg/m^3 isopycnal depths along with their standard deviations are presented. The 25.8 kg/m^3 and 26.2 kg/m^3 isopycnal depths help define several recurring patterns (Figures 8 and 9). Over the continental shelf and slope the internal density field mimics the bathymetry. The isopycnals shoal onshore from the slope region. Depth contours are aligned nearly parallel to the coastline with sharpest gradients near the shelf break-slope region. These gradients relax in the Gulf of the Farallones and in Monterey Bay.

34

West of the continental shelf and upper slope are three prominent meander and/or eddy structures. The implied geostrophic flow around these three features is anticyclonic. The southernmost structure appears as a closed eddy centered west of Monterey Bay and extending down to where the 26.2 kg/m^3 isopycnal deepens to at least 110 meters. This feature will be called the Monterey Bay eddy. A second structure appears at the western boundary of the survey region, centered west of the Half Moon Bay to Pescadero region, near the Pioneer Seamount area. This feature will be called the Pioneer eddy. The 26.2 kg/m^3 isopycnal reaches a depth of a least 130 meters in the Pioneer eddy. The northern-most eddy structure also appears at the western boundary of the survey region and is centered west of Bodega Bay. This feature will be called the Bodega eddy. The Bodega eddy is associated with a deepening of the 26.2 kg/m^3 isopycnal to 120 meters. Isopycnal depth contours extending offshore of and aligned with Pt. Reyes form a wedge shape which divides the Bodega eddy from the Pioneer eddy.

Standard deviations of the 25.8 kg/m^3 isopycnal depth (Figure 10) show highest variability in the northern portion of the survey area, offshore from Pt. Reyes, with lower standard deviations appearing in the southern region and within the Gulf of the Farallones. This is due to sharpest gradients occurring in the Pt. Reyes upwelling filament region with deepest isopycnals just offshore of the filament. Standard deviations of the 26.2 kg/m^3 isopycnal depth (Figure 11) show highest deviations in the same northern region off Pt. Reyes, along with high deviations in the Monterey Bay region and in a region west of the shelf off Half Moon Bay.
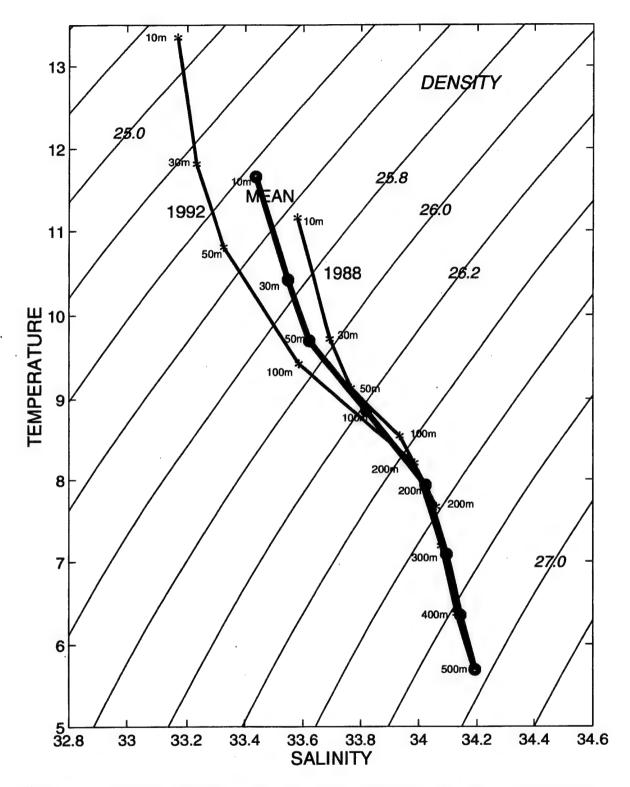
Figure 7. TS Diagrams for the 10 year mean (1987-1996) along with the two contrasting years of 1988 and 1992. Bold circles and asterisks along the TS curves denote the values at discrete depths from 10 to 500 meters.
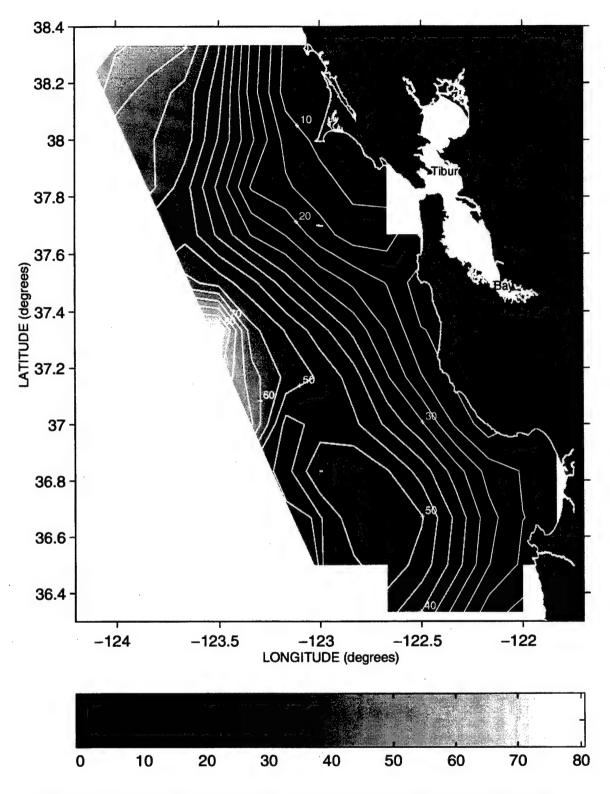
Figure 8. Mean depths of the 25.8 kg/m^3 isopycnal during May-June, 1987-1996.
Contour interval is 5 meters.

37
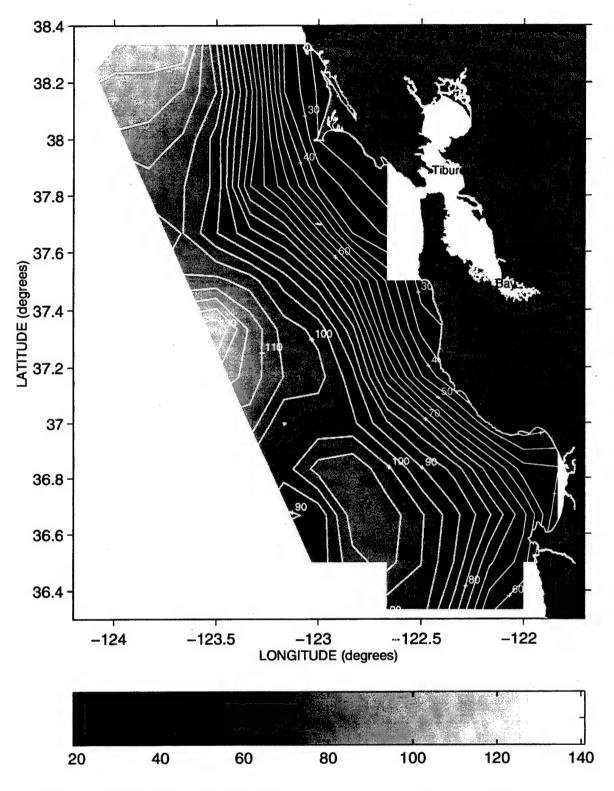
Figure 9. Mean depths of the 26.2 kg/m^3 isopycnal during May-June, 1987-1996. Contour interval is 5 meters.
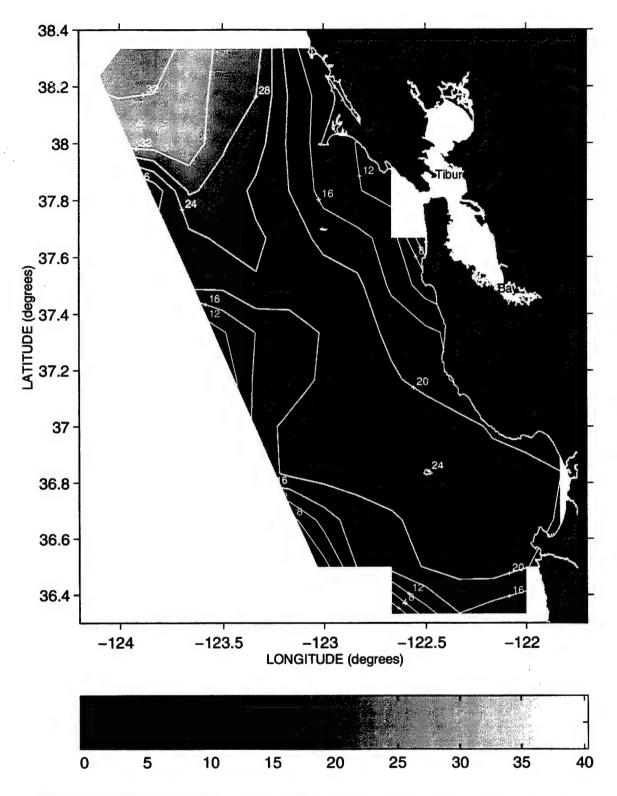
Figure 10. Standard deviations of the 25.8 kg/m^3 isopycnal depths during May-June, 1987-1996. Contour interval is 4 meters.
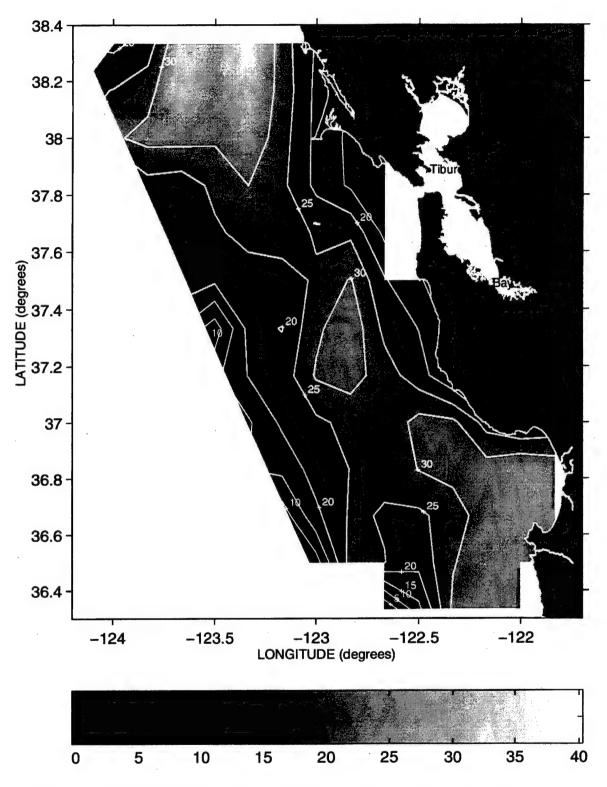
Figure 11. Standard deviations of the 26.2 kg/m³ isopycnal depths during May-June, 1987-1996. Contour interval is 5 meters.

To determine water mass characteristics in the upper ocean, the salinity on the 25.8 and 26.2 isopycnals was examined. Horizontal contour charts of salinity climatologies on these two density surfaces along with contour charts of the standard deviations of salinity are presented in Figures 12, 13, 14, and 15. On both surfaces, salinities increase monotonically over the continental shelf so that highest salinity is found at the coast. With respect to alongshore variability at the coast, highest salinities on both isopycnals occurred near Bodega Bay, in the northern section of the Gulf of the Farallones, and along the shore from Pescadero to Monterey. This higher salinity water inshore and over the shelf is the product of coastal upwelling of subsurface water which has a higher percentage of subtropical water. Signatures for the three offshore meander-eddy structures are present in these salinity fields with minima at their cores. These contour charts define a pattern of recirculating higher salinity water from the continental shelf region around the Monterey Bay eddy. The two offshore meander-eddy structures north of the Monterey Bay eddy show different water mass characteristics from that of the Monterey Bay eddy. The lower salinities of the two northern structures indicate that the source of water for these two meanders or eddies is the relatively fresh Pacific Subarctic water located in the CC which is west of the survey area. The positions of the three meander-eddy structures appearing in the salinity fields correspond to those appearing in the isopycnal depth charts. Horizontal contour charts of standard deviations for salinities on the two isopycnals are presented in Figures 14 and 15. Highest deviations occur at the upwelling regions around Pt. Reyes and Pt. Año Nuevo, and inside Monterey Bay. Smaller deviations occur offshore of the shelf.

41
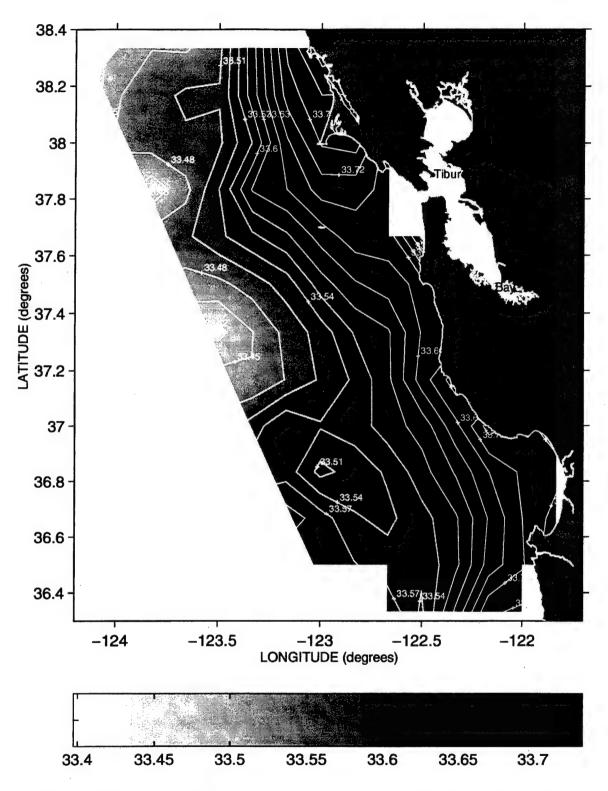
Figure 12. Mean Salinity (PSS) on the 25.8 kg/m^3 isopycnal during May-June, 1987-1996. Contour interval is 0.02.
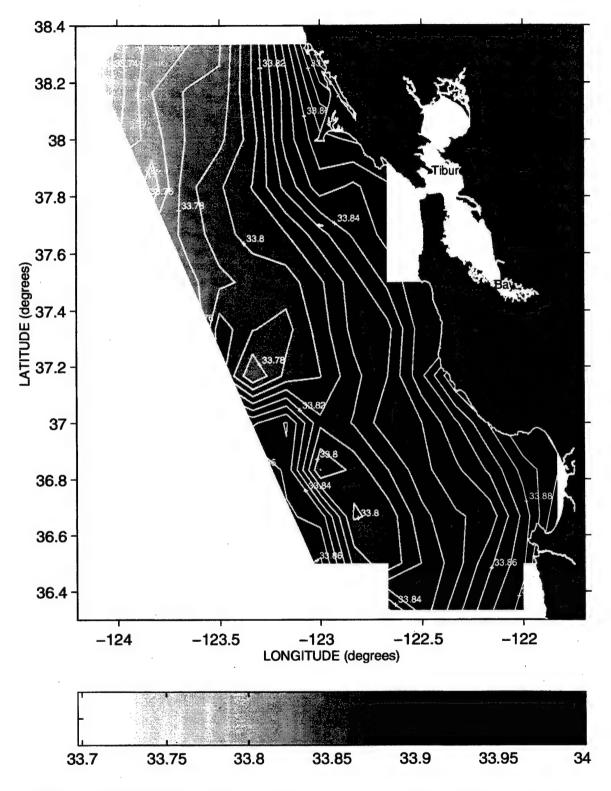
Figure 13. Mean Salinity (PSS) on the 26.2 kg/m³ isopycnal during May-June, 1987-1996. Contour interval is 0.01.
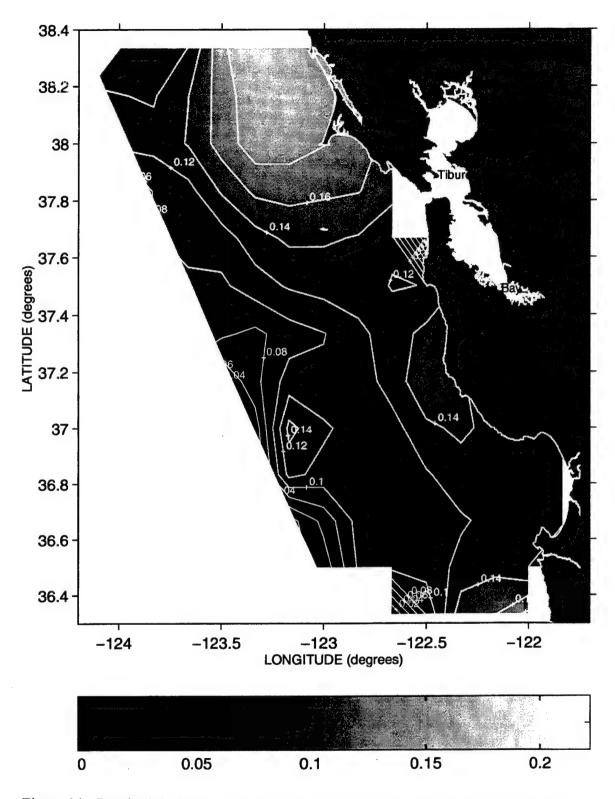
Figure 14. Standard deviations of the salinity on the 25.8 kg/m³ isopycnal during May-June, 1987-1996. Contour interval is 0.02.
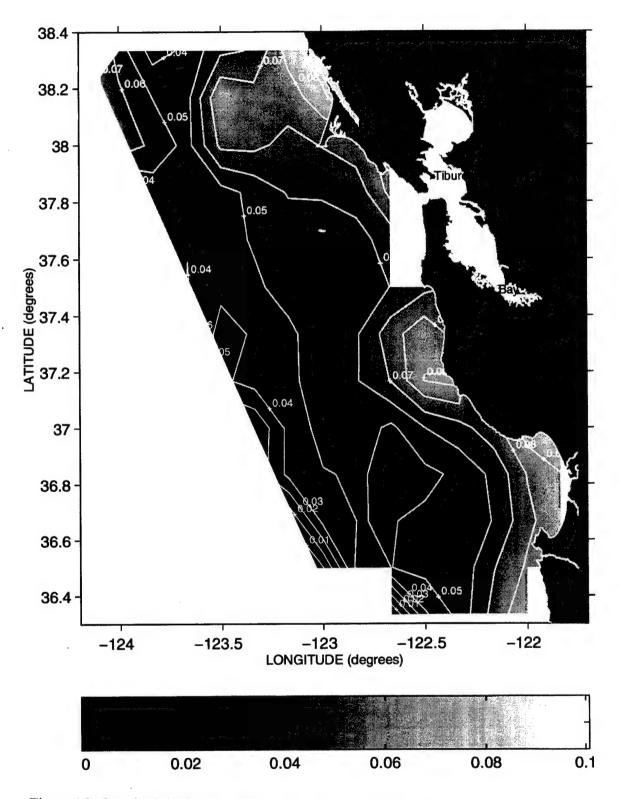
Figure 15. Standard deviations of the salinity on the 26.2 kg/m^3 isopycnal during May-June, 1987-1996. Contour interval is 0.01.

Climatologies of temperature, salinity and potential density at 30 meters along with their standard deviations are presented in Figures 16 through 21. Thirty meters is the depth at which nighttime midwater trawls were deployed during the May-June surveys in order to sample for juvenile rockfish. Contoured patterns and structures in these horizontal charts resemble the charts of depths and salinities at the 25.8 kg/m^3 and 26.2 kg/m^3 isopycnals. The continental shelf region contains cooler, saltier, and denser water than the areas west of the shelf. In all the variables at 30 meters, standard deviations are highest in the northwest region of the survey area off Pt. Reyes.

To assess the mean structure of the upper mixed layer, horizontal contour charts of the climatologies for the MLD were produced. Wind keeps water above the thermocline well mixed. Temperature and salinity tend to remain relatively stable within this mixed layer and wind generated turbulence is often present in the mixed layer as well. Figures 22 and 23 illustrate the climatological MLD patterns and standard deviations of the MLD. In general, a deeper mixed layer occurs in the northern region of the survey area with greatest depths offshore of the Bodega Bay to Pt. Reyes shoreline. Mixed layer depths are larger offshore than inshore for the majority of the survey area. These patterns probably result from a combination of circulation features, ocean water residence time and the wind field. Buoy climatologies (Figure 4) show that winds are typically stronger in the northern region of the survey area during the upwelling season, especially off Pt. Reyes. Nelson (1977) also showed that winds, based on ship observations over several decades, are stronger in the northern region of the survey area.
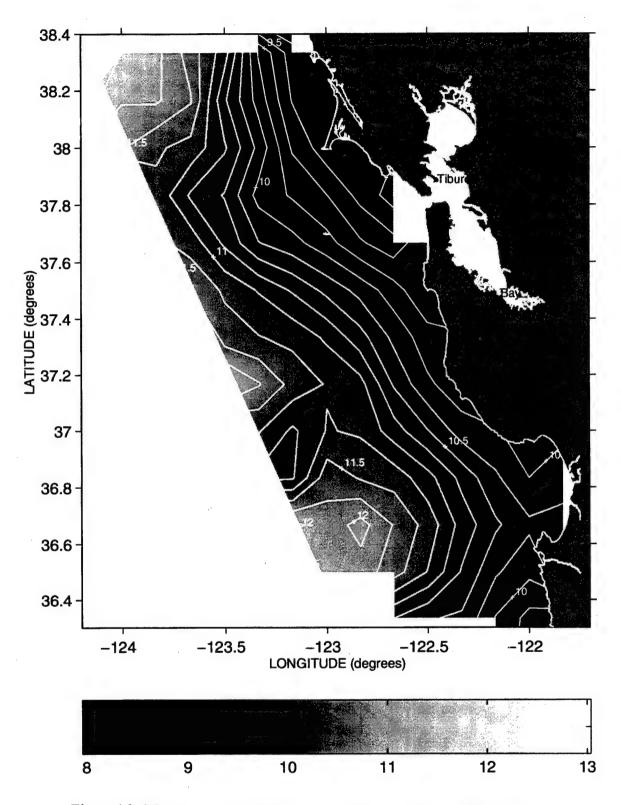
Figure 16. Mean temperature at 30 meters during May-June, 1987-1996.
Contour interval is 0.5° C.
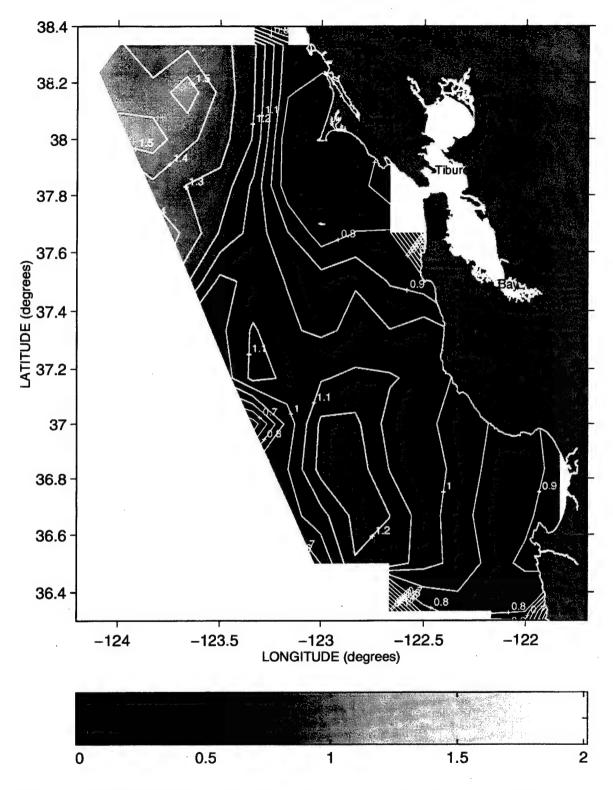
Figure 17. Standard deviations of the temperature at 30 m during May-June, 1987-1996. Contour interval is 0.1° C.
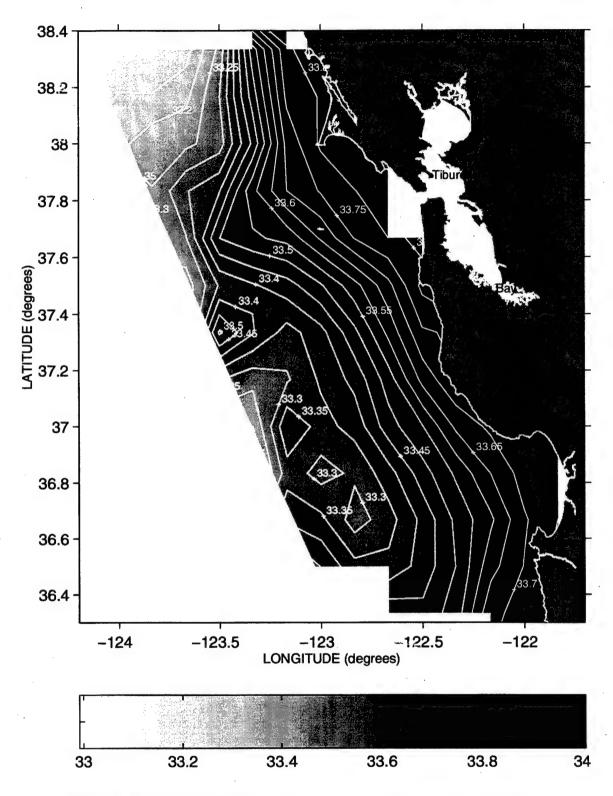
Figure 18. Mean salinity (PSS) at 30 meters during May-June, 1987-1996.
Contour interval is 0.05.
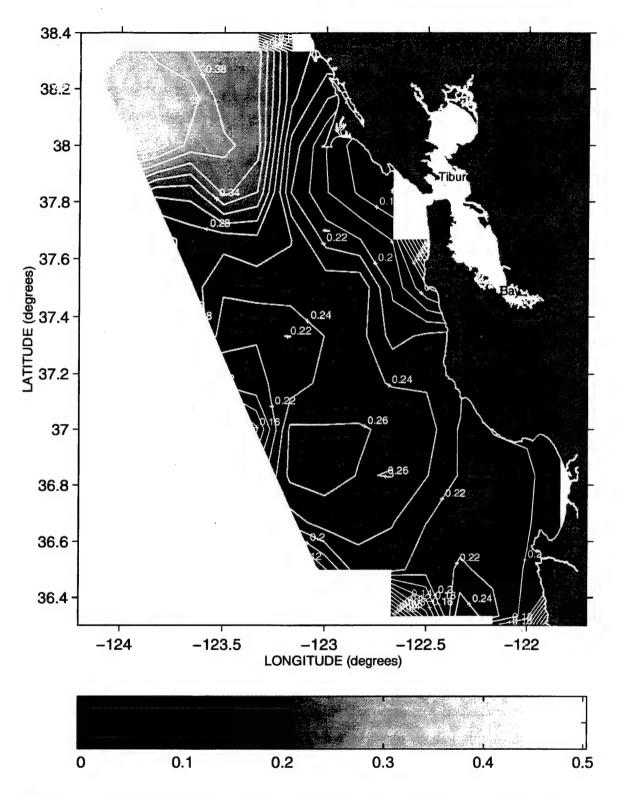
Figure 19. Standard deviations of salinity at 30 meters during May-June, 1987-1996. Contour interval is 0.02.
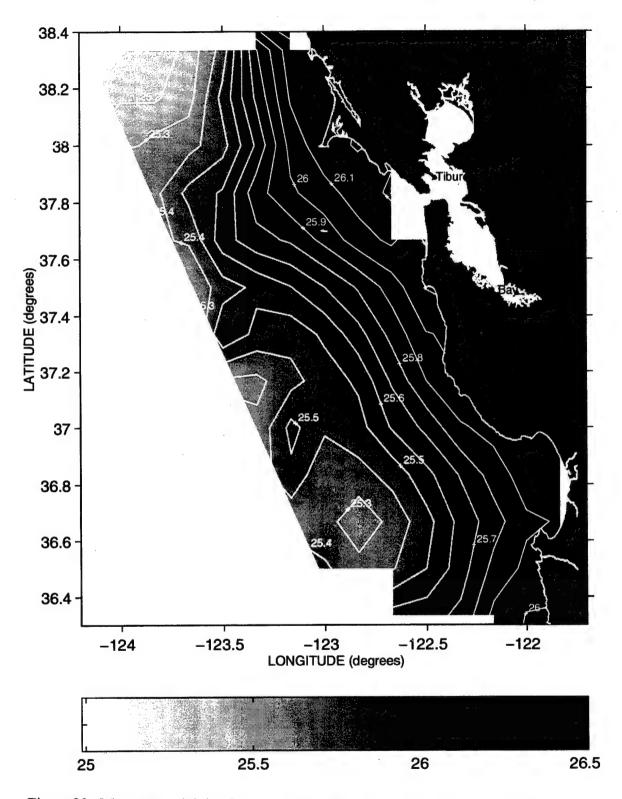
Figure 20. Mean potential density anomaly at 30 meters during May-June, 1987-1996.
Contour interval is 0.1 kg/m³.
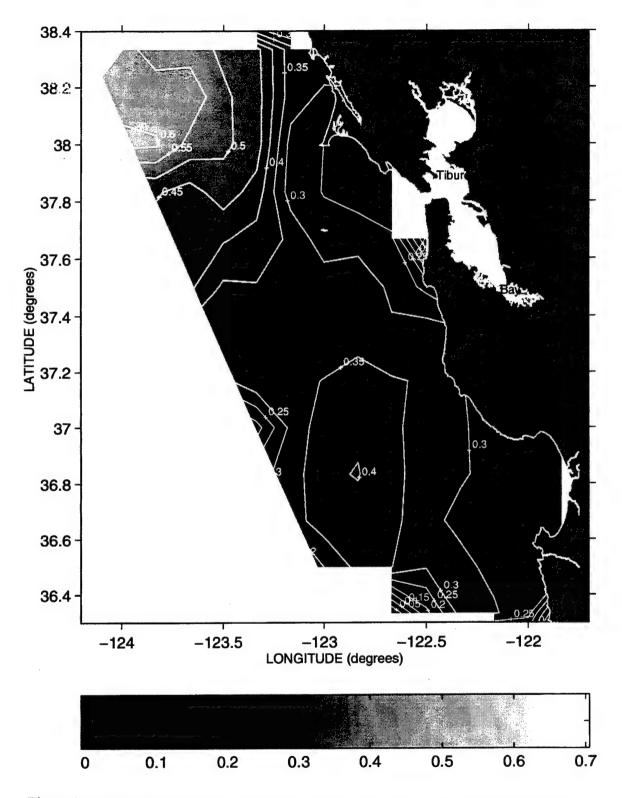
Figure 21. Standard deviations of potential density anomaly at 30 meters during May-June, 1987-1996. Contour interval is 0.05 kg/m³.
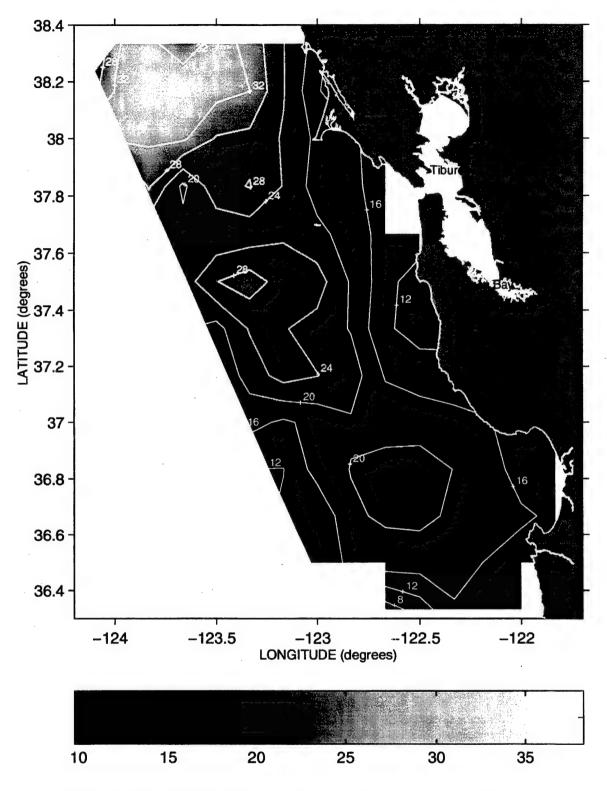
Figure 22. Mean depths of the mixed layer during May-June, 1987-1996.
Contour interval is 5 meters.

53
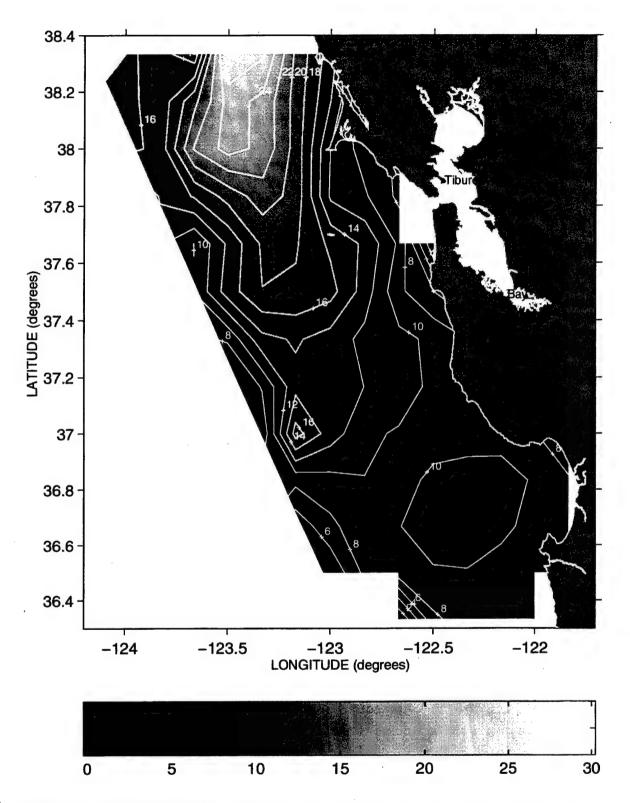
Figure 23. Standard deviations of the mixed layer depth during May-June, 1987-1996.
Contour interval is 2 meters.

54

B. VARIABILITY

Plots of buoy alongshore wind, buoy SST, SEFI SST, and SEFI SSS from January through June of each year between 1987 and 1996 (Appendix A) show the significant variability that these oceanographic variables undergo before and during the survey period. Selected plots from different years are presented as examples in Figures 24, 25, and 26. In each of these figures and in Appendix A, the light gray shaded area and bold-dotted line represent the climatology and normal variance.

Figure 24 illustrates the alongshore wind variability during the first half of 1993. Wind velocities and directions are highly coherent throughout the survey region. Significant relaxations and reversals of equatorward winds occurred during the first two sweeps of the survey period with strong equatorward winds returning during sweep 3. Frequencies of equatorward wind relaxations/reversals ranged from 3 to 20 days.

Figure 25 illustrates SST during the first half of 1996 at the four buoys. Buoy SSTs have a high positive correlation but are not as highly coherent as buoy measured alongshore winds. 1996 SSTs showed high variability during the spring and summer months. The spring months were relatively warm and the summer months during the survey period were anomalously cold. These cold SSTs were due to the extremely persistent and strong equatorward winds occurring during sweeps 2 and 3.

Figure 26 illustrates sea surface temperature and sea surface salinity at SEFI during the first half of 1991 and 1992, two highly contrasting years. 1991 was anomalously cold and salty during the survey period whereas 1992, an ENSO year, was anomalously warm and fresh.

Alongshore Winds from NOAA NDBC Buoys ~ 1993

Buoy 46013 ~ Bodega, CA

PCA direction = 132 degrees

Buoy 46026 ~ Gulf of the Farallones, CA

PCA direction = 128 degrees

Buoy 46012 ~ Half Moon Bay, CA

PCA direction = 152 degrees

Buoy 46042 ~ Monterey Bay, CA

PCA direction = 148 degrees
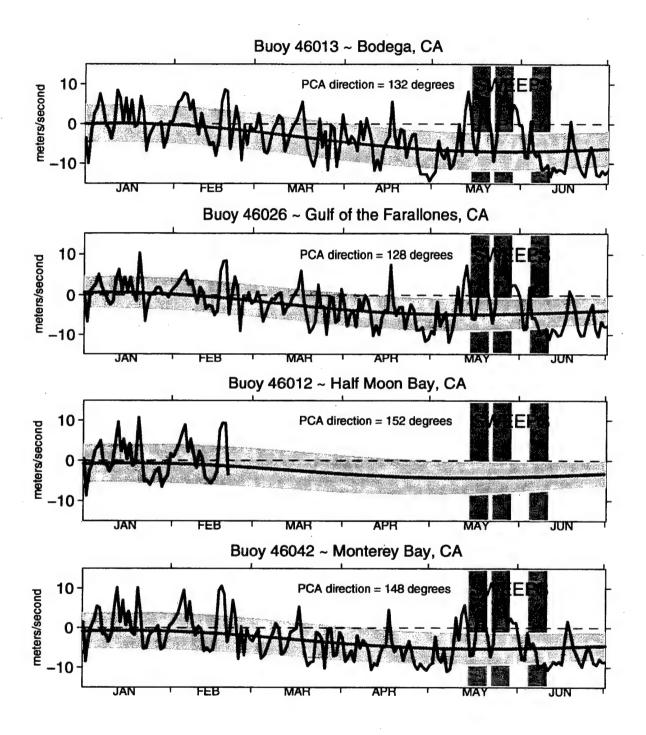
Figure 24. Buoy alongshore winds during the first six months of 1993.

Sea Surface Temperatures from NOAA NDBC Buoys ~ 1996
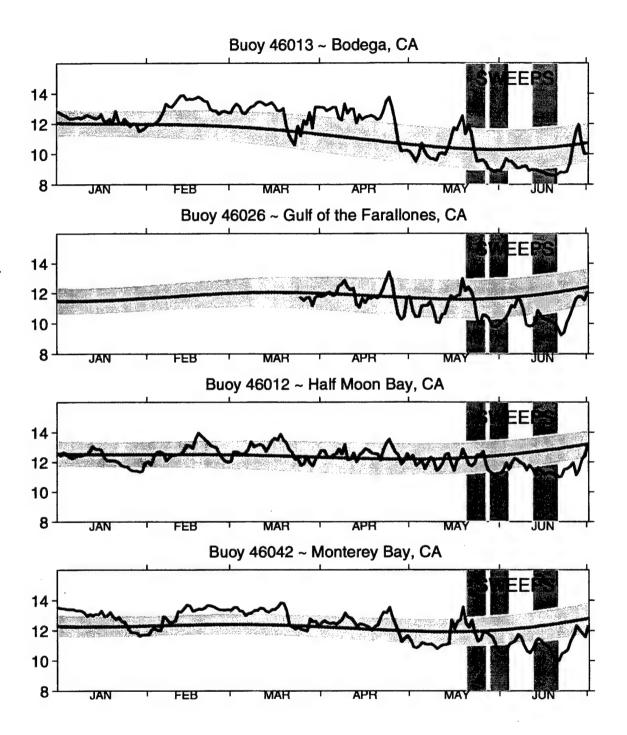
Figure 25. Buoy SSTs during the first six months of 1996, SSTs are in degrees Celsius.

Temperature and Salinity at Southeast Farallon Island

Sea Surface Temperature ~ 1991

Surface Salinity ~ 1991

Sea Surface Temperature ~ 1992

Surface Salinity ~ 1992
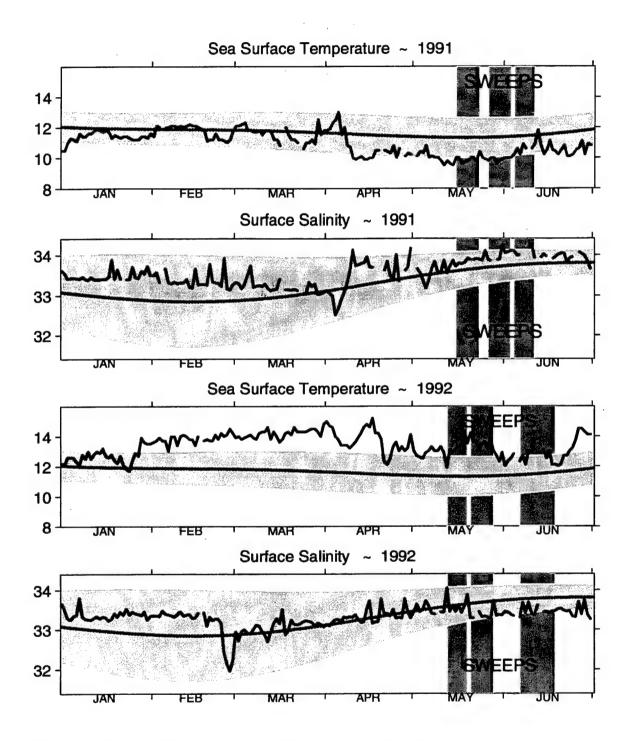
Figure 26. SST and SSS at Southeast Farallon Island during the first six months of 1991 and 1992. SST is in degrees Celsius and SSS is from the practical salinity scale.

58

Subsurface temperature, salinity and density values at discrete depths during all ten annual surveys are presented in Figure 27. In general, upper ocean waters in 1987, 1988, 1989, and 1996 were cool and salty. 1990 was a slightly fresh year down to 100 meters and salty at greater depths. 1991 and 1994 were cool years with 1994 being fresh below 50 meters. 1995 was cool and fresh down to 200 meters. 1992 and 1993 (2 ENSO years) were characterized as extremely warm and fresh on pressure surfaces. On density surfaces, 1987-1989 and 1996 were warm and saline (spicy), while 1990-1995 were generally cool and fresh.

Horizontal contour charts of the surveys' CTD variables for the 30 sweeps from 1987-1996 were produced (Appendix B). Marked variability in the CTD variables (depth and salinity at the 25.8 kg/m^3 and 26.2 kg/m^3 isopycnals, mixed layer depth) occurred from both year to year and from sweep to sweep. Figures 28, 29, and 30 serve as examples that illustrate both the inter-annual and inter-sweep variability in the depth of the 25.8 kg/m^3 isopycnal. Figure 28 is a contoured chart of the 25.8 kg/m^3 isopycnal depths during the first sweep of 1992, an ENSO year. The entire survey region contained relatively "light" water in the upper 100 meters of the water column, as evidenced by the relatively deep locations of the 25.8 kg/m^3 isopycnal. Contrasting this are the relatively shallow locations of the 25.8 kg/m^3 isopycnal during an equivalent period during 1996 (Figure 29). Figure 29 illustrates 25.8 kg/m^3 isopycnal depths during the first sweep of 1996 and shows evidence of much denser water in the upper water column than during the first sweep of 1992. Comparisons of Figure 29 (sweep 1, 1996) with Figure 30 (sweep 3, 1996) helps illustrate the variability between sweeps of an individual year.. Water is denser overall during the third sweep than during the first sweep. Anomalously strong upwelling during the third sweep of 1996 caused

59

the 25.8 kg/m^3 isopycnal to shoal within a very large region around Pt. Reyes, into the Gulf of the Farallones, and from the Pescadero to Davenport nearshore area. Shoaling of the 25.8 kg/m^3 isopycnal was not as widespread during the first sweep of 1996. In general, upwelling conditions in the upper water column (cool, saline, dense) within the survey area, especially over the continental shelf, were more "mature" at the conclusion of the cruises than at the beginning.
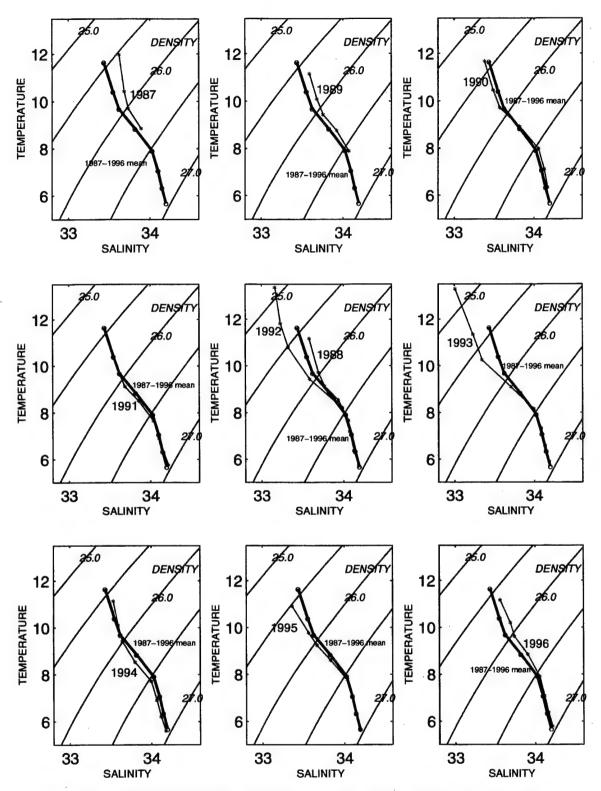
Figure 27. Temperature-Salinity diagrams for each of the annual May-June surveys, 1987-1996. The ten year mean values are plotted along with each of the yearly values.
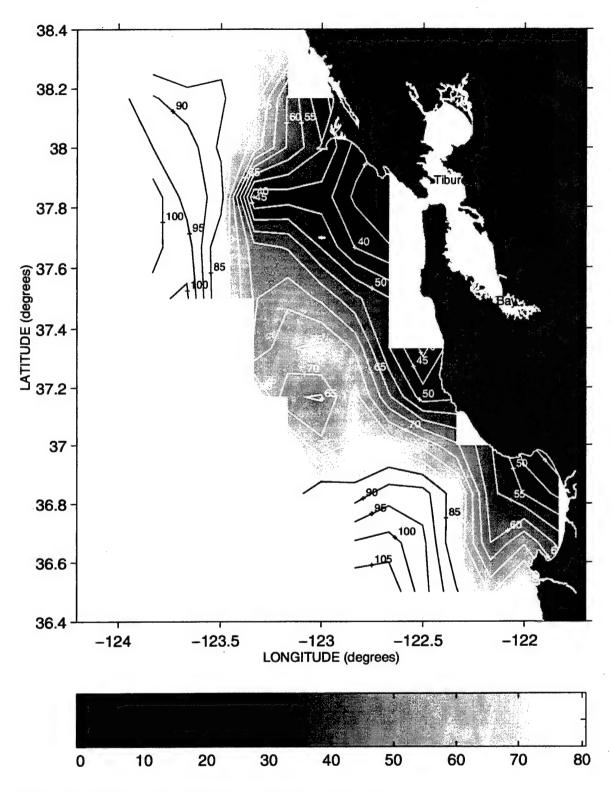
Figure 28. Depth of the 25.8 kg/m³ isopycnal during sweep 1, 1992. Contour interval is 5 meters. 1992 was characterized as an anomalously "light water" year.
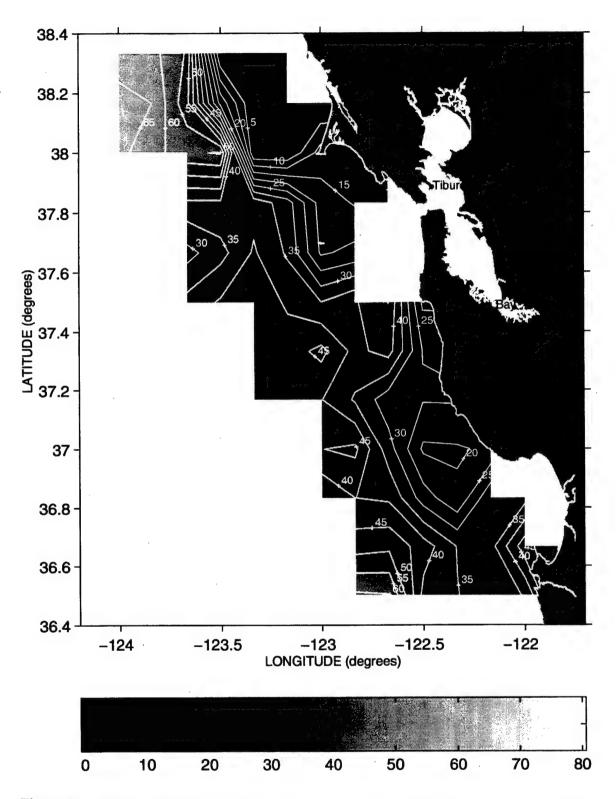
Figure 29. Depth of the 25.8 kg/m³ isopycnal during sweep 1, 1996. Contour interval is 5 meters. 1996 was characterized as having a strong upwelling season.
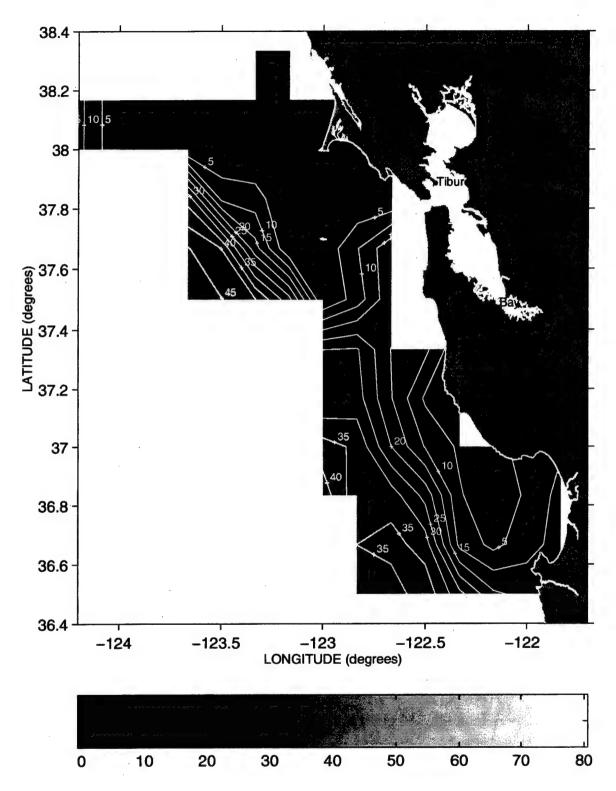
Figure 30. Depth of the 25.8 kg/m³ isopycnal during sweep 3, 1996. Contour interval is 5 meters. Shoaling of this isopycnal occurred in the region around Pt. Reyes.

Results from the EOF analysis of the CTD variables yielded three statistically and physically significant modes (EOFs) in each case (Figures 31-36). Significant modes are defined as those patterns which accounted for more than 5% of the total variance in the particular CTD variable. The first several EOFs are likely to represent geophysical signals. These modes have an extremely low probability of arising from random noise since their percentage of total variance explained is greater than 5%. Modes of variance that account for less than 5% of the total are likely due to noise. Each EOF spatial pattern for depth and salinity at the two density surfaces is presented as a single figure while the corresponding temporal amplitude functions of the first three modes are shown in a single figure.

The Zscore spatial patterns of the first EOF for the 25.8 kg/m^3 and 26.2 kg/m^3 isopycnal depths are shown in Figures 31 and 32 and their temporal amplitudes in Figures 37 and 38. These patterns represent 53% of the total variance for the 25.8 kg/m^3 isopycnal depth and 68% of the total variance for the 26.2 isopycnal depth. The spatial patterns are presented as horizontal contour charts with arbitrary units of depth. In both cases these contours of Zscores or eigenvectors produce an overall cross-shore gradient with the zero crossing (delineation between positive and negative Zscores) located parallel and close to the continental slope. It suggests two distinct regions: a nearshore region, which mimics the shape of the continental shelf, characterized by negative Zscores and an offshore region described by positive Zscores. Since the temporal amplitudes for these first modes are always positive (Figures 37 and 38), the negative and positive spatial Zscores represent shallower and deeper isopycnals, respectively. The lower amplitudes also represent a relaxation of isopycnal depth gradients.

The second EOFs for the 25.8 kg/m^3 and 26.2 kg/m^3 isopycnal depths have similar orientations in the spatial Zscore pattern and explain 17% (25.8 isopycnal depth) and 9% (26.2 isopycnal depth) of the residual variance. These EOF spatial patterns are shown in Figures 33 and 34. These second modal patterns exhibit alongshore structure and some cross-shore structure as well. Positive Zscores are generally found to the north and negative Zscores to the south. The second EOF for the 25.8 isopycnal depth also shows a cross-shore gradient off Pt. Reyes (Figure 33). The zero crossings are oriented in a northeast to southwest direction and are located in the Gulf of the Farallones region. In these cases, the spatial EOFs represent two distinct patterns because the amplitude time-series associated with this mode can be either positive or negative (Figures 37 and 38).

In both cases, the third EOF for the two isopycnal depths represents 6% of the total variance (Figures 35 and 36). Some prominent features in the spatial Zscore patterns appear to be manifestations of upwelling filaments, eddies, and meanders. The three prominent eddy-like features seen in the CTD climatologies appear in the spatial pattern for the 25.8 kg/m^3 isopycnal depth (Figure 35). The Pt. Reyes filament also shows up quite well in the spatial pattern with steep Zscore gradients off Bodega and Pt. Reyes and extending both offshore and into the Gulf of the Farallones. At the 25.8 kg/m^3 isopycnal depth, the Bodega and Pioneer eddies are in phase with each other, and the Pt. Reyes filament and Monterey Bay eddy are in phase.
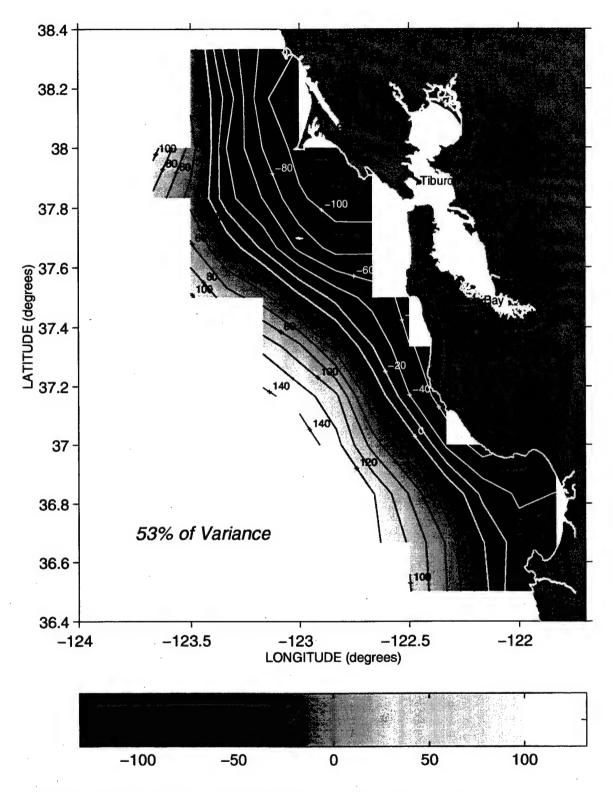
Figure 31. Zscore pattern of the first EOF mode for the 25.8 kg/m^3 isopycnal depth.
Contour interval is 20.
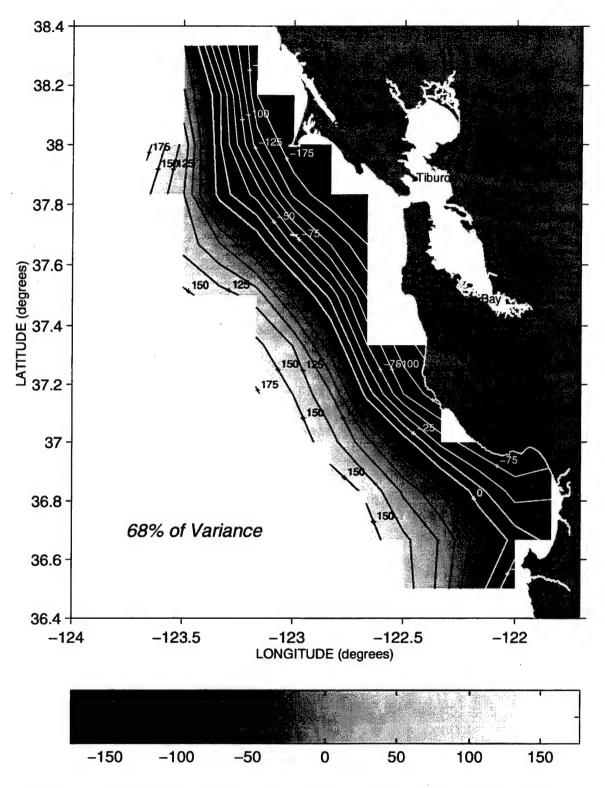
Figure 32. Zscore pattern of the first EOF mode for the 26.2 kg/m³ isopycnal depth.
Contour interval is 25.
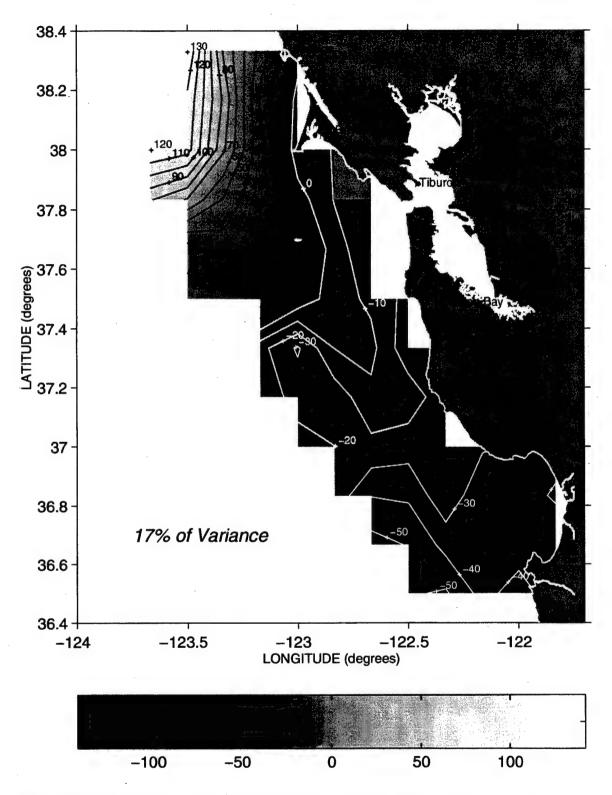
Figure 33. Zscore pattern of the second EOF mode for the 25.8 kg/m^3 isopycnal depth. Contour interval is 10.
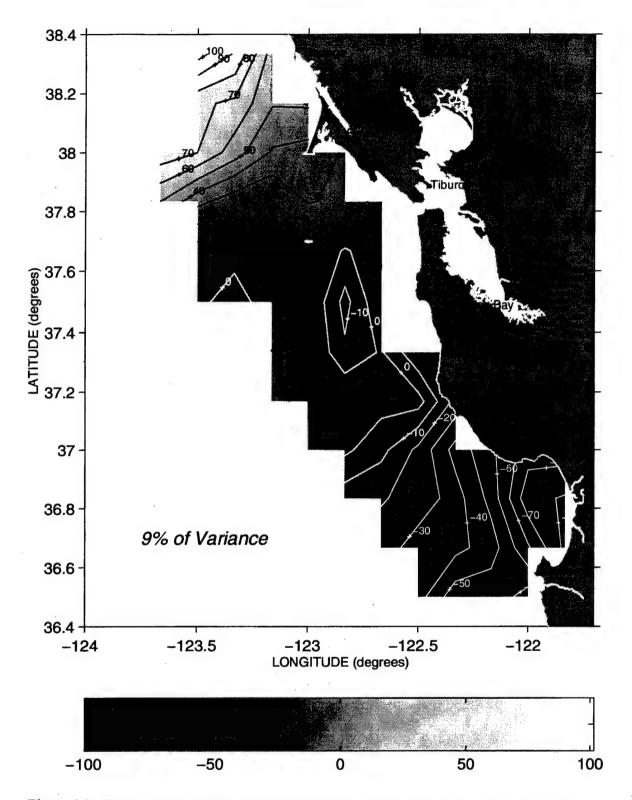
Figure 34. Zscore pattern of the second EOF mode for the 26.2 kg/m^3 isopycnal depth. Contour interval is 10.
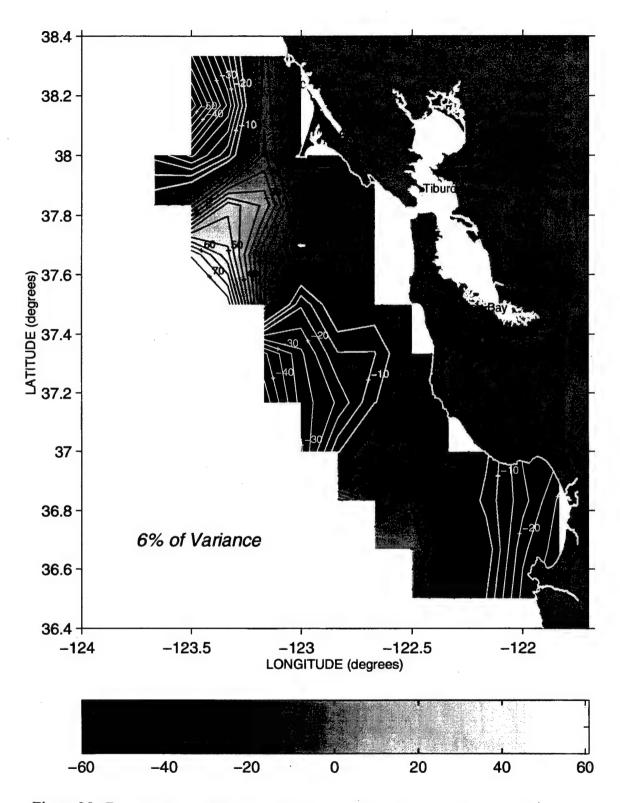
Figure 35. Zscore pattern of the third EOF mode for the 25.8 kg/m^3 isopycnal depth. Contour interval is 5.
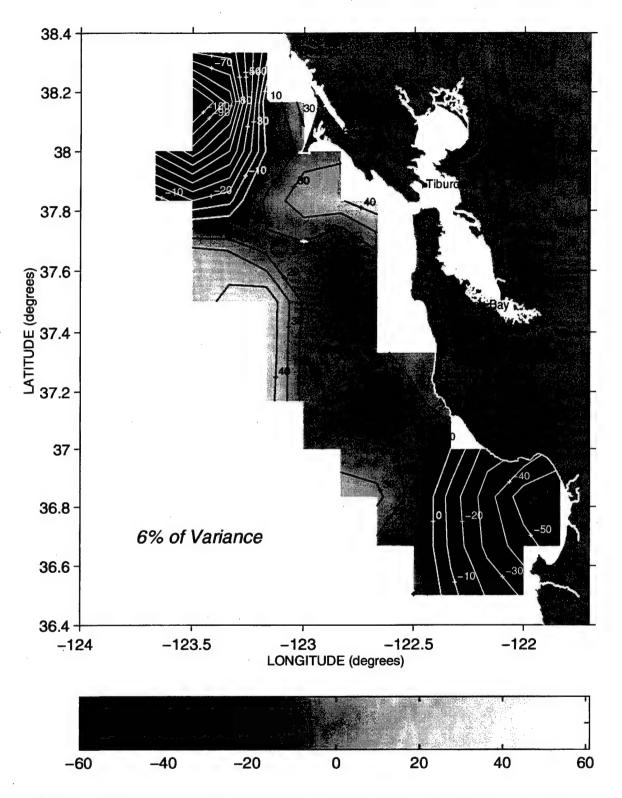
Figure 36. Zscore pattern of the third EOF mode for the 26.2 kg/m^3 isopycnal depth. Contour interval is 5.
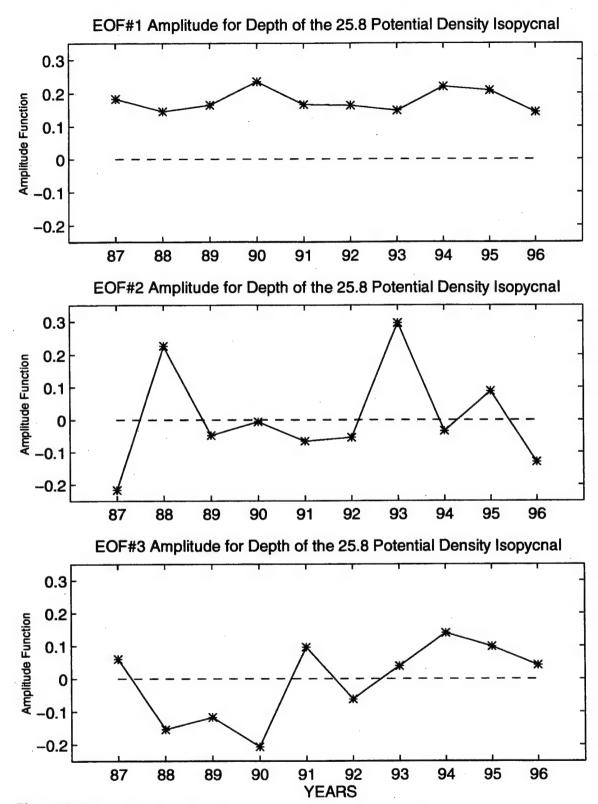
Figure 37. Temporal amplitudes of the first three EOF modes for the 25.8 kg/m³ isopycnal depth.
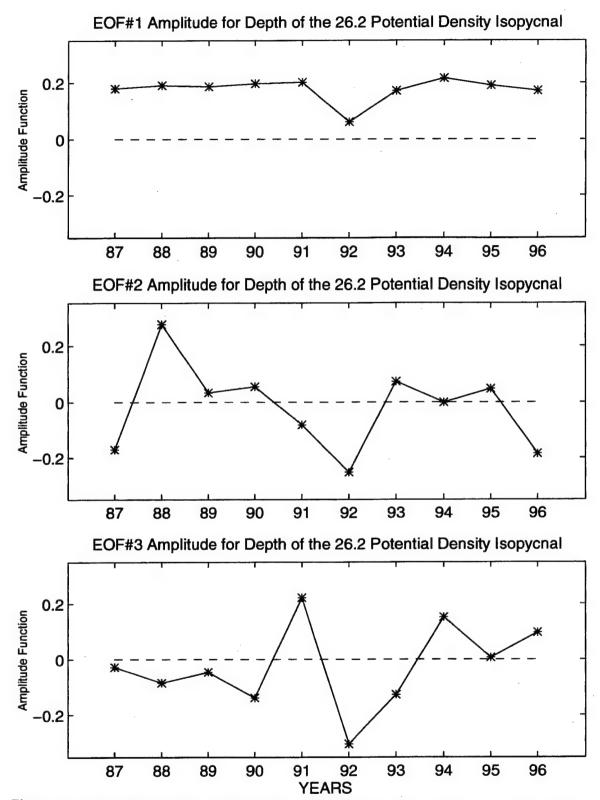
Figure 38. Temporal amplitudes of the first three EOF modes for the 26.2 kg/m^3 isopycnal depth.

The first EOF for salinity on the 25.8 kg/m³ and 26.2 kg/m³ isopycnals is shown in Figures 39 and 40 and their temporal amplitudes in Figures 45 and 46. These patterns represent 48% of the total variance for salinity on the 25.8 kg/m³ isopycnal and 46% of the total variance for salinity on the 26.2 kg/m³ isopycnal. The spatial patterns are presented as horizontal contour charts with arbitrary units of salinity. In both cases these contours of Zscores or eigenvectors produce an overall cross-shore pattern. The zero crossing for salinity at the 25.8 kg/m³ isopycnal was located parallel and close to the continental slope except in the southern portion of the Gulf of the Farallones, where the zero crossing bent towards the shoreline around Half Moon Bay (Figure 39). The zero crossing for first mode of salinity at the 26.2 kg/m³ isopycnal was located closer to shore in the northern section of the survey area and farther offshore in the southern region (Figure 40). The structure of the spatial pattern exhibited a significant cross-shore variation in the salinities. It suggests two distinct regions as did the first mode EOF for isopycnal depths: a nearshore region, characterized by positive Zscores, indicative of saltier water and an offshore region described by negative Zscores, indicative of fresher water. Since the temporal amplitudes for these first modes were always positive (Figures 45 and 46), the negative and positive spatial Zscores represent fresher and saltier water, respectively.

The second EOF for the salinity on the 25.8 kg/m³ and 26.2 kg/m³ isopycnals had similar orientations in the spatial Zscore pattern and these patterns explained 17% (25.8 isopycnal salinity) and 16% (26.2 isopycnal salinity) of the residual variance (Figures 41 and 42). These second modal patterns exhibited alongshore structure and some cross-shore structure as well. Negative Zscores were generally found to the north around Pt. Reyes and

75

into the Gulf of the Farallones and positive Zscores to the south. The second EOF for salinity on isopycnals also showed a cross-shore oriented pattern in the Zscore contours off Pt. Reyes. The zero crossing for the second EOF of the 25.8 kg/m^3 isopycnal salinity was oriented in a northeast to southwest direction and was located in the Gulf of the Farallones region (Figure 41). The zero crossing for the second EOF of the 26.2 kg/m^3 isopycnal salinity was oriented in an east to west-northwest direction and was located in the Gulf of the Farallones region. This zero crossing clearly delineated the Pt. Reyes upwelling area and the Gulf of the Farallones from the regions to the south. In both isopycnal salinity cases, the spatial EOFs represented two distinct patterns because the amplitude time-series associated with this mode can be either positive or negative (Figures 45 and 46). This is similar to what was seen with the second mode EOF amplitudes for the depths of isopycnals.

In both cases, the third EOF for the two isopycnal salinities represented 6% of the total variance (Figures 43 and 44). One prominent feature that was resolved in the spatial Zscore patterns for both isopycnals is the Pt. Reyes upwelling filament, which extended southwest from Pt. Reyes through the western boundary of the survey area. Another significant feature in this third spatial EOF for the 25.8 kg/m^3 isopycnal depth was the appearance of the Bodega eddy which was out of spatial phase with the Pt. Reyes filament. Again the temporal amplitudes modulated between positive and negative values, and the Zscores in the spatial patterns changed sign accordingly.

76
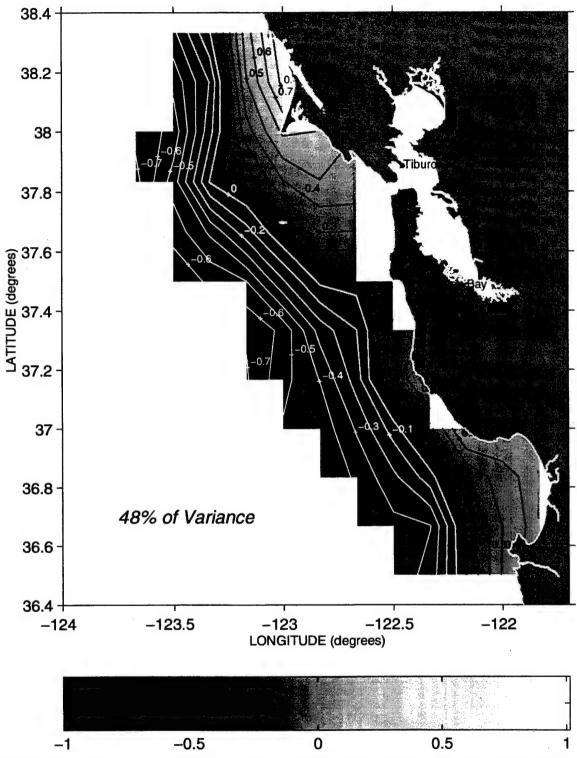
Figure 39. Zscore pattern of the first EOF mode for salinity on the 25.8 kg/m^3 isopycnal. Contour interval is 0.1.
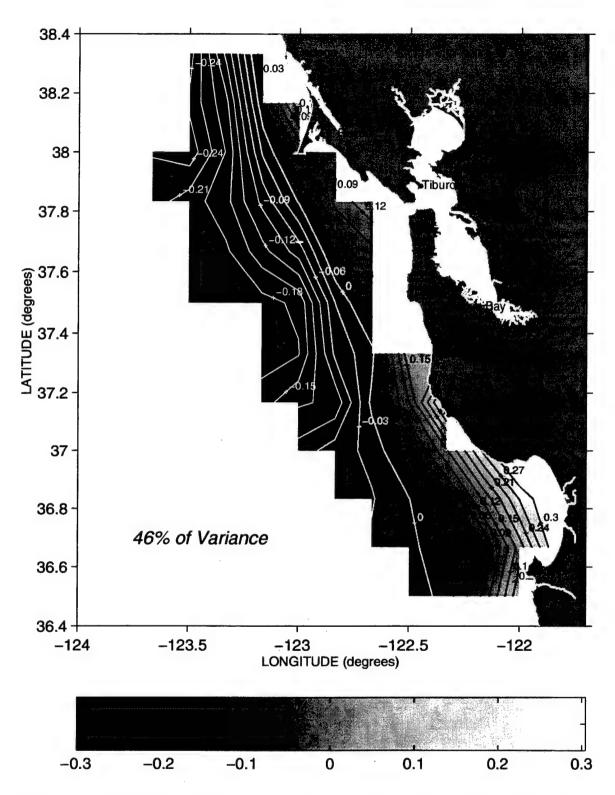
Figure 40. Zscore pattern of the first EOF mode for salinity on the 26.2 kg/m³ isopycnal.
Contour interval is 0.03.
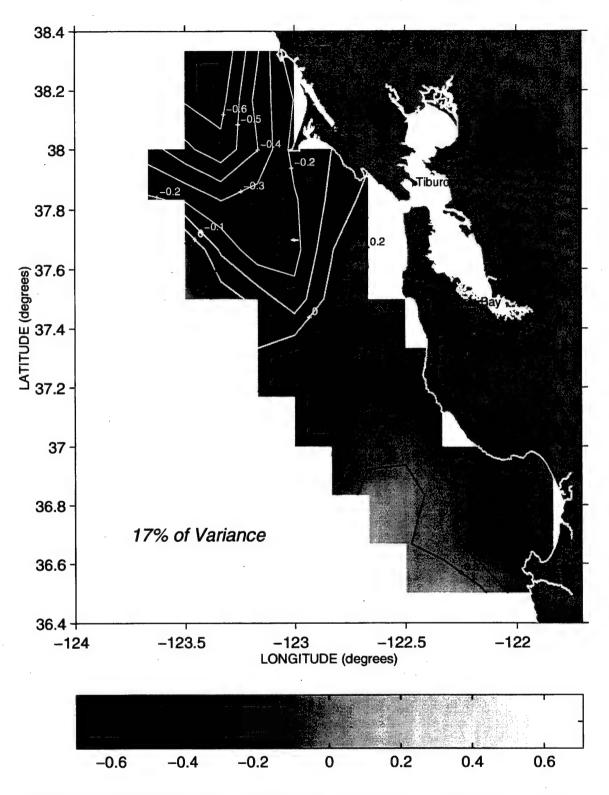
Figure 41. Zscore pattern of the second EOF for salinity on the 25.8 kg/m^3 isopycnal. Contour interval is 0.1.
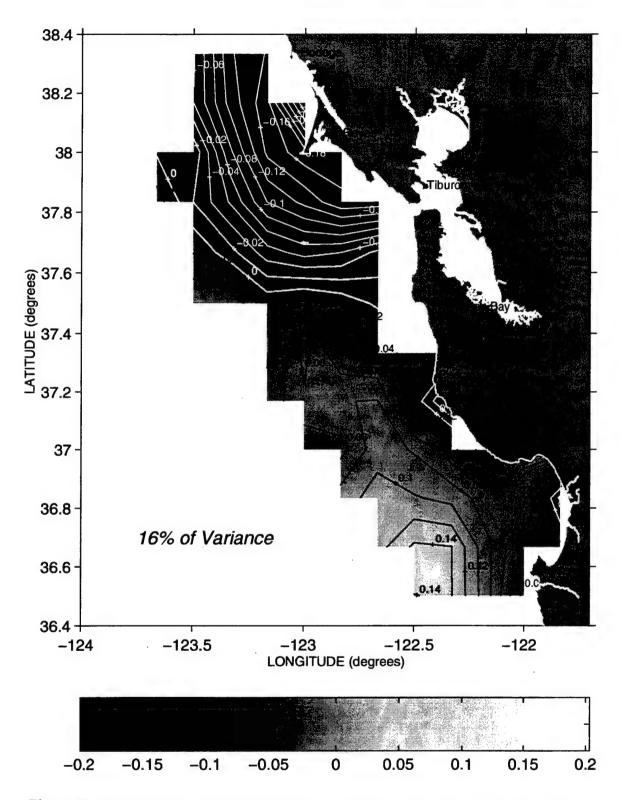
Figure 42. Zscore pattern of the second EOF for salinity on the 26.2 kg/m^3 isopycnal. Contour interval is 0.02.
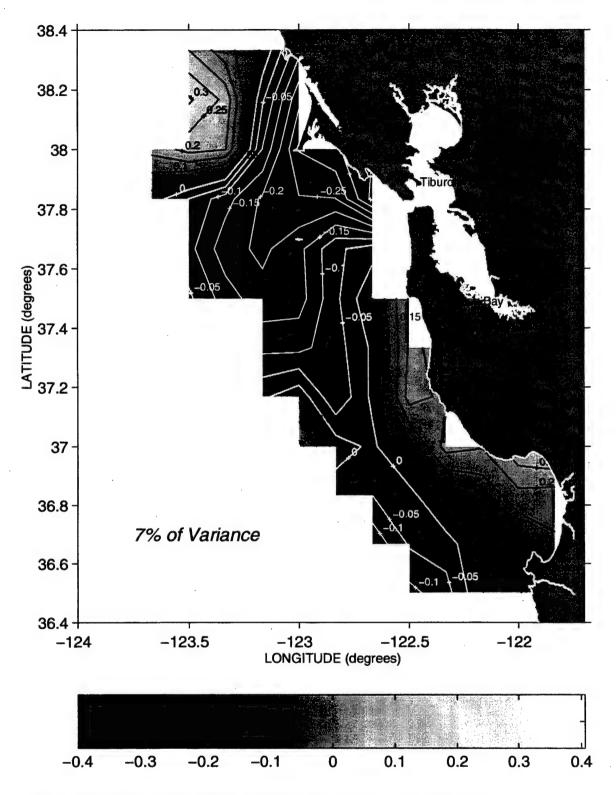
Figure 43. Zscore pattern of the third EOF for salinity on the 25.8 kg/m^3 isopycnal. Contour interval is 0.05.
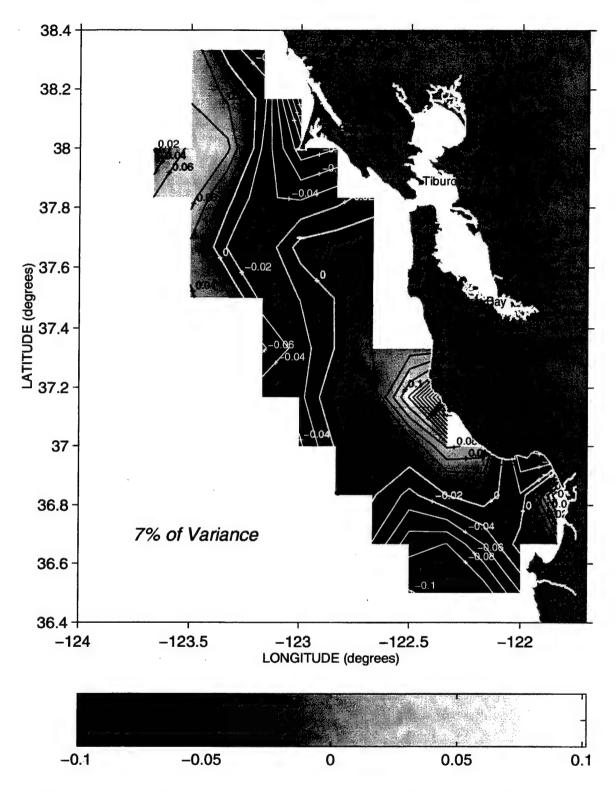
Figure 44. Zscore pattern of the third EOF for salinity on the 26.2 kg/m^3 isopycnal. Contour interval is 0.02.
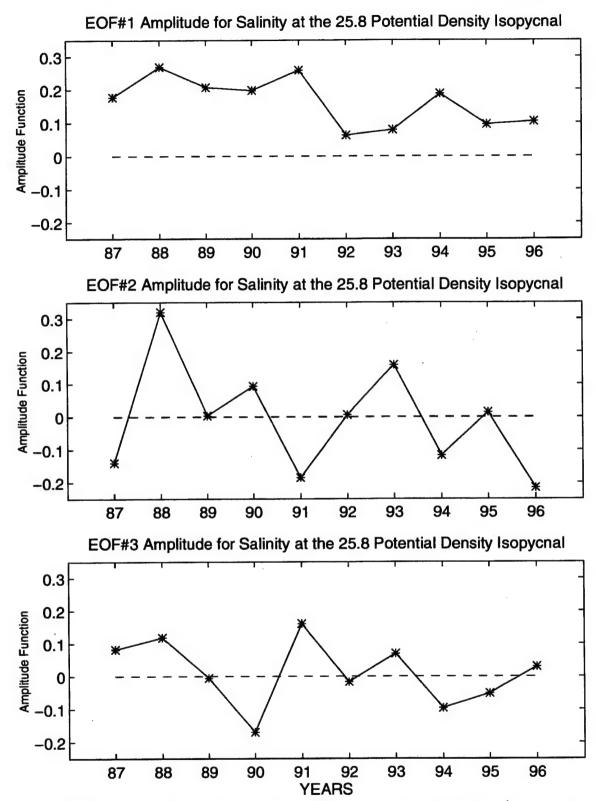
Figure 45. Temporal amplitudes of the first three EOFs for salinity on the 25.8 kg/m³ isopycnal.
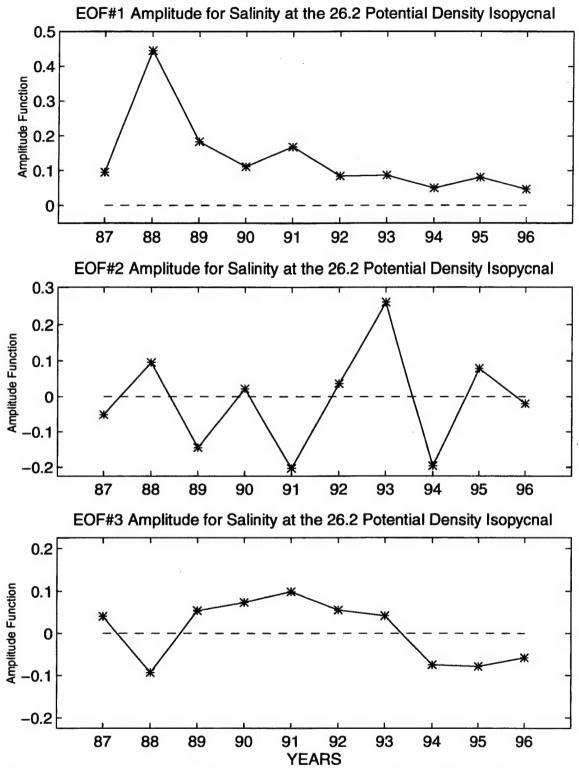
Figure 46. Temporal amplitudes of the first three EOFs for salinity on the 26.2 kg/m³ isopycnal.

V. DISCUSSION

A.   SURFACE CONDITIONS

Distinct seasonalities were apparent in the alongshore wind and SST measured by the four NOAA weather buoys in the survey area. Climatological analysis of the buoy data since the early 1980's showed that maximum equatorward winds and lowest sea surface temperatures occurred during May-June, the period of the NMFS surveys. Climatological analysis of the SST and SSS data collected over the last 70 years from Southeast Farallon Island showed that lowest SST and maximum SSS occurred during the May-June period. Based on these results, **the height of the upwelling season off central California occurs during May-June**.

Variability on a synoptic time scale in these seasonal surface conditions was quite evident when considering the daily data against a climatological background (Appendix A). The oscillating behavior of persistent equatorward alongshore wind and wind relaxation events plays a important role in producing variability in SST and SSS during the upwelling season. Wind relaxation events (i.e., a wind reduction or reversal) were seen to occur at intervals between 3 and 20 days during May and June. Upwelling favorable winds brought denser water to the surface which was cooler and saltier. Accompanying this upwelling was Ekman transport of the denser water in a seaward direction into the buoys' and Farallon Islands' regions. Wind relaxation events discontinued this upwelling process and associated offshore Ekman transport.

Variability in surface conditions also occurred on an interannual time scale. This can

85

be seen by comparing years with stronger than normal upwelling favorable winds and years with lower than normal, or downwelling favorable winds (e.g., 1996 vs. 1993). Anomalous surface conditions that are manifestations of large scale eastern North Pacific ocean conditions and/or remotely forced phenomena produced interannual variability as well. An excellent example of this is the anomalously warm and fresh conditions observed in 1992 that were associated with the 1991-1993 El Niño-Southern Oscillation effect (Sakuma et al., 1992, 1993; Ramp et al., 1997; Armstrong, 1996). The warming and freshening which occurred in the survey region during 1992 and 1993 was most likely caused by an onshore transport of warmer, fresher offshore California Current waters and an ensuing depression of the thermocline (Lynn et al., 1995). This mechanism has been previously suggested as the cause of coastal warming off California during the 1940-41, 1982-83, and 1992-93 ENSO events (Simpson, 1984).

B.   SUBSURFACE CONDITIONS

Climatologies of the CTD variables indicate some prominent and robust features in the circulation dynamics and water mass characteristics. Over the continental shelf and slope areas, isopycnal contour plots defined an internal density field that mimicked the shelf-slope bathymetry with isopycnals shoaling nearshore and becoming deeper offshore. This was representative of a coastal upwelling signature with a much denser (cooler and saltier) nearshore zone bordering a lighter (warmer, fresher) offshore region. The inshore, exceptionally dense water was associated with well known persistent upwelling locales near Pt. Reyes, Pt. Año Nuevo, and just south of the survey area at Pt. Sur (Huyer and Kosro, 1987; Brink and Cowles, 1991; Kelly, 1985; Breaker and Mooers, 1986; Schwing et al.,

86

1991; Breaker and Broenkow, 1994; Parker, 1996). Greater offshore Ekman transport with generally stronger upwelling in the north results in the advection of denser water further offshore, and the difference in area covered by the upwelled water is usually greater in the north around Pt. Reyes than to the south.

Other prominent features that appeared in the climatologies of the internal density fields were the three robust eddy structures located seaward of the continental shelf. The relatively light water at the cores of these eddies and the contoured patterns of isopycnal depths implies anticyclonic flow for each eddy. The northernmost eddy is centered west of Bodega Bay and the centrally located eddy is near the Pioneer Seamount area. These two northern eddies appeared to extend deeper than the eddy to the south. The southern-most eddy off Monterey Bay displayed a well defined anticyclonic circulation around a low salinity core within the bounds of the survey area. A significant result from examining the mean salinities at the two isopycnals is the water mass property differences between the Monterey Bay eddy and the two northern eddies. The higher overall mean salinities on isopycnal surfaces on the offshore side of the Monterey Bay eddy suggested that denser, spicier nearshore-shelf water was being advected clockwise around this eddy structure. The lower salinity values in the two northern eddies suggested that fresher, offshore California Current water of Pacific Subarctic origin was entrained in these eddies. The Monterey Bay eddy has been previously described (Rosenfeld et al., 1994; Strub et al., 1991) with its formation ascribed to the vorticity imparted by upwelling filaments from the Pt. Año Nuevo upwelling center to the north and from the Pt. Sur upwelling center to the south. The formation was also ascribed to a flow pattern that geostrophically adjusts to differences in water mass

densities. However, the fundamental difference in water masses between the Monterey Bay eddy and the eddies directly north of it have heretofore not been described. The most significant difference is that the Monterey Bay eddy is formed and maintained by coastal upwelling and filament vorticity while the two northerly eddies appear within the survey area by onshore movements of meanders and /or eddies from the eastern edge of the California Current

The other significant feature in the climatologies of the internal density fields was the upwelling filament off Pt. Reyes. This filament was quite persistent during May and June and extended offshore in a west-southwest direction creating a wedge of dense water which separated the two northern offshore eddies. The Pt. Reyes filament was observed in the vast majority of sweeps over the ten years from 1987-1996. The vertical and horizontal structure, along with subsurface velocities, of this filament have been described by Parker (1996) and Steger (1997). This filament remains persistent during the upwelling season over a range of wind conditions, even during prolonged relaxation events. Thus the flow in the Pt. Reyes filament was not driven by variations in Ekman transport alone. This persistent filament appears to be driven by a combination the local wind curl and non-linear responses to the topography of the local coastline.

C.   EOF INTERPRETATIONS

Even though EOF analysis is a popular application for analysis of climate variability in the oceanographic and meteorological communities, there exists little standard of objectivity for the interpretation of the representative EOF modes. Results of an EOF analysis are inherently subjective, yet many investigators neglect to identify their interpretive

approach. The approach used here was similar to that suggested by Armstrong (1996): each EOF modal Zscore spatial pattern and temporal amplitudes were used together to describe the variability. The zero crossing of Zscores in the spatial patterns appear to have geophysical significance, but of greater importance is the relative change of the spatial Zscores (positive vs. negative values). Each of the spatial modes are discussed within the context of the mesoscale regional oceanography.

EOF analysis of the internal density field based on the depth of and salinity on the 25.8 kg/m^3 and 26.2 kg/m^3 potential density anomaly surfaces yielded three significant modes, which together, accounted for the vast majority of the variance in the ten years of CTD data for those variables. Patterns of variability within the upper water column dynamics, such as geostrophic flow parallel to isopycnal contours and vertical movement of isopycnals in response to wind stress and wind stress curl can be deduced by interpreting the EOFs for isopycnal depth. Patterns of variability in water mass properties can be resolved by interpreting the EOFs for salinity on the isopycnal surfaces.

The spatial pattern for the first EOF mode for both the depth of and salinity on the two isopycnals displays an overall alongshore orientation in Zscore contours with gradients having a cross-shore orientation. These patterns represent 53% of the total variance for the 25.8 kg/m^3 isopycnal depth, 68% of the total variance for the 26.2 kg/m^3 isopycnal depth, 48% of the total variance for salinity on the 25.8 kg/m^3 isopycnal, and 46% of the total variance for salinity on the 26.2 kg/m^3 isopycnal. Zero crossings for first EOF modes of all the four variables were located in close proximity to and nearly parallel with the continental slope.

89

The nearshore region was invariably denser (higher salinities) with shallower isopycnals than the offshore region. This cross-shore pattern was consistent throughout the ten years from 1987-1996 because the corresponding temporal amplitudes remained positive. The overall cross-shore pattern was representative of a seasonal coastal upwelling signature with denser water developing in the upper water column over the shelf region with upward sloping isopycnals and lighter water and downward sloping isopycnals occurring west of the shelf.

A couple of patterns in the temporal amplitudes are worthy of mention (Figures 37 and 38). Amplitudes of first mode EOFs for isopycnal depths remained relatively stable throughout the ten years, which probably reflects the year to year consistency in the coastal bathymetry and upwelling season equatorward winds. There was a larger drop in the amplitude for the 26.2 kg/m^3 isopycnal depth during the ENSO year of 1992 due to an anomalous reduction in coastal upwelling. Amplitudes of first mode EOFs for salinity on the 25.8 kg/m^3 isopycnal showed an overall downward trend through the ten years with an especially large drop in the ENSO year of 1992. It is important to keep in mind that low temporal amplitudes are indicative of reduced cross-shore structure and more homogeneous density conditions, a probable manifestation of decreased upwelling rates, while higher amplitudes are a result of increased upwelling and larger lateral density gradients.

The spatial pattern for the second EOF mode for both depth of and salinity on the two isopycnals define two regions in an alongshore sense. These second mode EOF patterns explained 17% of the total variance for the 25.8 kg/m^3 isopycnal depth, 9% of the total variance for the 26.2 kg/m^3 isopycnal depth, 17% of the total variance for salinity on the 25.8

kg/m^3 isopycnal, and 16% of the total variance for salinity on the 26.2 kg/m^3 isopycnal. In the northern region of the survey area the second mode spatial Zscores always had the sign opposite to the sign for spatial Zscores in the southern region, with a zero crossing located generally south of the Gulf of the Farallones. These second EOF modes actually represent two distinct spatial patterns because, unlike the first mode, the associated temporal amplitudes change sign throughout the ten years.

The similar spatial variability structure present in all of the second EOF modes may represent a mesoscale flow separation between the northern region of the survey area and the southern region. A mechanism explaining such a pattern would be regional specific wind relaxation: if upwelling favorable winds were to relax or reverse more rapidly in the southern region than in the northern or vice versa, one could expect a regional heterogeneity in the coastal density signature. For example, a stronger relaxation event south would manifest itself in a cessation of the upwelling process, while upwelling still continued, at perhaps a reduced state, to the north. The antithesis of this first scenario may be the case when the temporal amplitudes change sign from one year to the next. This could be the result of increased upwelling in the southern region relative to the northern region. This north-south heterogeneity in "upwelling strength" has also been postulated by Armstrong (1996) as being a mechanism underlying the second EOF mode spatial pattern in AVHRR satellite sensed SST off central California.

However, other causes for the second EOF mode spatial pattern can be considered. Send et al. (1987), in a study of temperature evolution along the continental shelf between Pt. Reyes and Pt. Arena, suggested that warming north of Pt. Reyes during relaxation events

was related to solar heating of the surface mixed layer combined with poleward alongshore advection. Apparently, remote advection of warmer water from as far south as San Francisco occurred, although the exact nature of the forcing mechanism was not conclusive. Poleward flow along the shelf and slope has been described earlier by Chelton (1987), Tisch et al. (1992), Collins et al. (1996) and Steger (1997). The Tisch et al. and Steger results were unusual in that poleward flow occurred off Pt. Sur (Tisch et al., 1992) and off the Gulf of the Farallones (Steger, 1997) during a time of local equatorward wind stress. Remote wind forcing from the south was postulated as the mechanism for this phenomenon. Hickey (1979) suggested that late summer/early fall bursts of warmer poleward surface flow along central California could be the result of the increasing importance of positive wind stress curl during a period of diminishing equatorward wind stress. The wind curl field is positive throughout the year off central California (Bakun and Nelson, 1991), and through Sverdrup balance, such a positive wind curl would impose a net poleward flow. Interestingly, three of the four CTD variables show large positive spikes in their second EOF mode temporal amplitudes in 1993 which coincides with a period having a significant and prolonged relaxation event and poleward flow near the surface (Armstrong, 1996).

The spatial patterns for the third EOF mode for both depth of and salinity on the two isopycnals resolve the Pt. Reyes upwelling filament and offshore meander-eddy structures, and their possible connections. These third mode EOF patterns explain 6% of the total variance for the 25.8 kg/m^3 isopycnal depth, 6% of the total variance for the 26.2 kg/m isopycnal depth, 7% of the total variance for salinity on the 25.8 kg/m^3 isopycnal, and 7% of the total variance for salinity on the 26.2 kg/m^3 isopycnal. The spatial Zscore pattern of the

third EOF mode for the 25.8 kg/m^3 isopycnal depth shows the locations and spatial phasing characteristics of several robust features in the upper water column. These are the Pt. Reyes upwelling filament, the Bodega eddy, the Pioneer eddy, and the Monterey Bay eddy.

The spatial Zscore signs within each of these features illustrate the spatial phasing characteristics with zero crossings delineating the boundary around each of the features. The Bodega eddy in the northwest region of the survey area and the Pioneer eddy off Half Moon Bay are in phase. The Pt. Reyes filament is oriented in a southwest and offshore direction south of the Bodega eddy with relaxed gradients spreading southeasterly into the Gulf of the Farallones. This filament has the same sign (same phase) as the Monterey Bay eddy which is located in the southwestern region of the survey area.

The likely mechanism explaining these patterns and their phasing is a combination of coastal upwelling, offshore Ekman transport, eddy generation from filament vorticity, and onshore transport during relaxation events. During upwelling favorable winds the powerful Pt. Reyes filament develops and streams offshore of the survey area where its vorticity helps generate or strengthen the anticyclonic Bodega eddy. During these upwelling favorable wind periods the Monterey Bay eddy develops similarly off the mouth of the Monterey Bay. Ekman transport of surface waters during these periods help keep the two northern eddy (Bodega and Pioneer) signatures to the west of the survey area. However, the Monterey Bay eddy generally remains within the bounds of the survey area.

During wind relaxation events the two northern eddies rebound towards the shore due to a readjustment of the weakening cross-shelf pressure gradient. This onshore movement of the eddies will transport entrained, lighter, offshore water into the survey area. The region

within Monterey Bay is of the same sign and phasing as the two northern eddies. This is plausible if one considers that the Monterey Bay eddy will rebound onshore during relaxation events (Rosenfeld et al., 1994). This onshore movement Monterey Bay eddy would likely result in advection of offshore type waters into the Monterey Bay. There is much anecdotal evidence of offshore plankton species infiltrating shallower nearshore regions during wind relaxation events (Roughgarden et al., 1991; Bakun, 1996; Dan Howard, personal comm.). These offshore species are seen nearshore within half a day after strong equatorward winds relax, which corresponds closely to the local inertial period.

Acoustic Doppler Current Profiler (ADCP) vector data from the 1993 survey cruise described by Parker (1996) gives an excellent illustration of the phasing and location characteristics of the Pt. Reyes filament with the Monterey Bay eddy and the location-phasing characteristics of the two northern eddies along with the onshore eddy rebounding behavior during a relaxation event. A significant relaxation event occurred during sweeps 1 and 2 of the 1993 survey. The two northern eddies showed strong anticyclonic circulation ADCP vector patterns similar to that implied by the negative spatial Zscore patterns of the EOF analysis which also correspond to the two northern eddies (Figures 47 and 48). Water was also seen being advected into Monterey Bay during sweeps 1 and 2. These features have a warm near-surface signature, presumably indicating the presence of CC water. Their direction of circulation is consistent with the downward displacement of isopycnals in the center, as shown in the CTD data, and the positive mode of the third mode EOF Zscores (Figure 35). When upwelling favorable winds returned during sweep 3 of 1993 the ADCP vectors displayed patterns which were strikingly similar to the negative phase of spatial

94

Zscore patterns of the Pt. Reyes filament and Monterey Bay eddy, namely a strong jet flowing south and offshore from the Pt. Reyes area, and a strong anticyclonic circulation around the location of the Monterey bay eddy (Figure 49).

Third mode EOF temporal amplitudes for the salinity on the 25.8 kg/m^3 isopycnal were intriguing due to the high correlation they exhibited in relation to the total juvenile rockfish *(Sebastes spp.)* survey abundance indices (Figure 50). Perhaps this third mode EOF temporal amplitude is a proxy for important environmental linkages to the fisheries ecosystem. These environmental linkages are not well understood but are believed to play a significant role in determining year-class strength and distribution in fish species. These results from the analysis of hydrographic variability certainly act as a catalyst for further research on physical-biological interactions in coastal habitats.
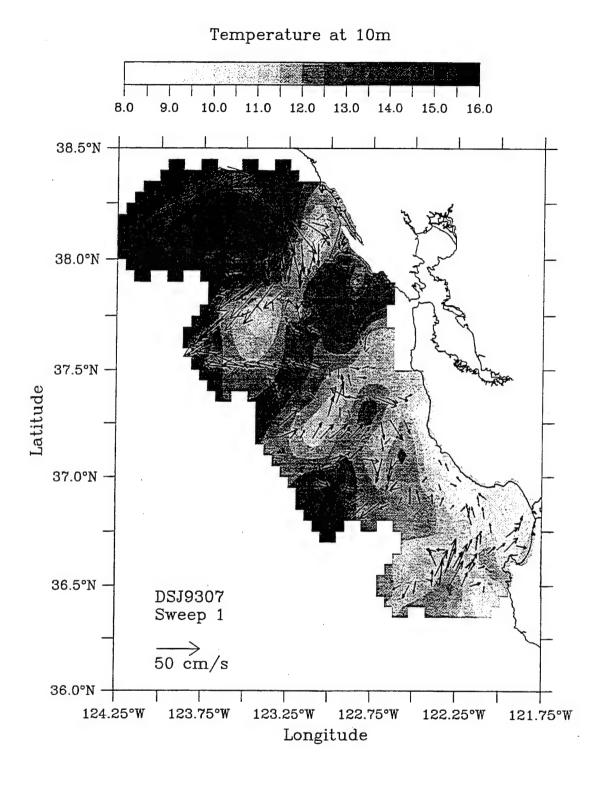
Figure 47. ADCP velocity vectors between 15-30 m and temperature (Celsius) at 10 m during sweep 1, 1993. Adapted from Parker (1996).

Figure 48. ADCP velocity vectors between 15-30 m and temperature (Celsius) at 10 m during sweep 2, 1993. Adapted from Parker (1996).
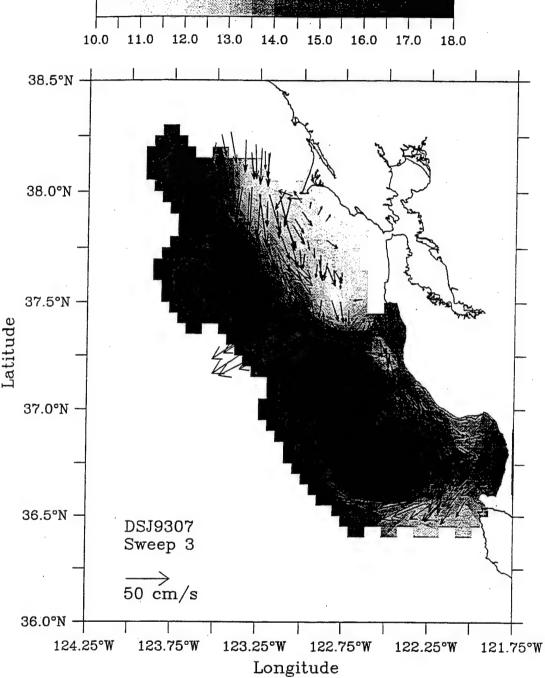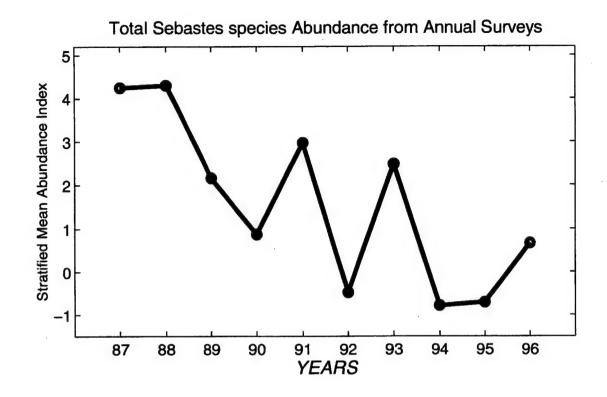
Figure 49. ADCP velocity vectors between 15-30 m and temperature (Celsius) at 10 m during sweep 3, 1993. Adapted from Parker (1996).
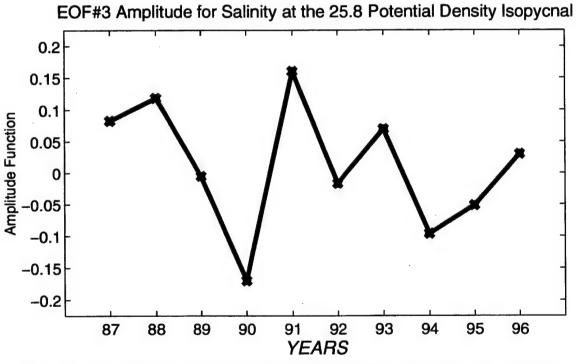
Figure 50. Total juvenile rockfish abundances from annual surveys (top) and the third mode EOF temporal amplitudes for the salinity on the 25.8 kg/m^3 isopycnal (bottom). Adapted from Schwing et al., 1997.

VI. CONCLUSIONS

Analysis of mean conditions and variability during the upwelling season off central California was performed on data sets of CTD measurements from NOAA NMFS juvenile rockfish surveys and NOAA buoy and Southeast Farallon Island shoreline surface time series. The region between Point Reyes and Cypress Point was surveyed with CTDs thirty times during May-June, 1987-1996. The analysis of these rich data sets has produced a conceptual model of hydrography and implied circulation for a unique eastern boundary current region of high productivity and biological diversity along an open coast.

Climatologies of alongshore wind, sea surface temperature, and sea surface salinity revealed that the height of the upwelling season occurred during the NMFS survey period. Variability in the surface conditions was high both inter-annually and inter-seasonally with maximum equatorward wind, lowest SST, and highest SSS occurring during May and June.

Ten year climatologies of late spring, subsurface hydrographic conditions from CTD data (depth and salinity on potential density anomaly surfaces, and temperature, salinity, density at discrete depths) indicate a complex signature of circulation patterns and water mass properties. The upper water column of the nearshore region was generally filled with relatively dense, upwelled water and isopycnal gradients conformed to the local bathymetry. A robust upwelling filament off Pt. Reyes appearing in the climatologies was generated and enhanced by local winds, yet remained persistent despite wind fluctuations. Seaward of the shelf break, three recurring anticyclonic eddy-like features appeared. The two northern eddy features were composed of relatively fresh California Current water from the offshore regions.

101

The southern-most eddy appeared to recirculate water that contained a relatively high portion of recently upwelled water.

An EOF analysis of depth at and salinity on discrete isopycnals to deduce subsurface variability patterns confirmed the prominent features that appeared in the climatologies. The EOFs represented patterns of spatial variability, whose seasonal evolution was reflected in the corresponding temporal amplitude time series. The geophysical signal of the first EOF-amplitude pairs represented a mean cross-shore upwelling pattern. The second EOF-amplitude pairs represented a geographically differing alongshore structure caused by spatial variations in the upwelling-favorable wind field and in alongshore gradients of water mass characteristics. The third EOF-amplitude pairs resolved the characteristics of the Pt. Reyes filament and the three eddies offshore of the continental shelf. The two northerly eddies appeared to be in phase and rebounded shoreward during wind relaxation events, transporting lighter (warmer, fresher) offshore water to the nearshore. The southernmost eddy and Pt. Reyes filament appeared to be in phase, intensifying during periods of upwelling favorable winds and diminishing during wind relaxation events. Future surveys could well resolve the western extent of the two northern eddies and the mixing interactions with the CC by extending the CTD stations westward from the eddy core locations.

The physical ramifications of the upwelling process in concert with coastal bathymetry exert a pivotal role in producing the complex distribution, movement and composition of ocean waters off the central California coast. EOF analysis of synoptic CTD data is an effective method for detecting and illustrating variability in subsurface conditions during the dynamic upwelling season. In the future, it should be possible to apply these methods in a

more thorough, multi-disciplinary study of environmental linkages to the marine ecosystem of the California coast. Such studies can lead to a better understanding of the reasons for species distributions and fluctuations as well as providing important information for natural resource management.

LIST OF REFERENCES

Armstrong, E.M., Spring-summer sea surface temperature variability off northern and central California from AVHRR satellite Imagery. M.S. Thesis, San Francisco State University, 1996.

Bakun, A., Patterns in the Ocean. California Sea Grant/CIB, 1996.

Bakun, A. and C.S. Nelson, The seasonal cycle of wind-stress curl in subtropical eastern boundary current regions. J. Phys. Ocean. 21:1,815-1834, 1991.

Botsford, L., The planktonic odyssey of larvae. California Sea Grant, R-041, 1996.

Bratkovich, A., R.L. Bernstein, D.B. Chelton, and P.M. Kosro, Central California coastal circulation study: program overview and representative results, in Southern California Bight Physical Oceanography, Proceedings of a Workshop, pp. 91-109, OCS Study MMS 91-0033, 1991.

Bray, N.A. and C.L. Greengrove, Circulation over the shelf and slope off northern California, J. Geophys. Res., 98, 18,119-18,145, 1993.

Breaker, L.C. and C.N.K. Mooers, Oceanic variability off the central California coast, Prog. Oceanog., 17:61-135, 1986.

Breaker, L. C. and W. W. Broenkow, The circulation of Monterey Bay and related processes. Oceanography and Marine Biology: an Annual Review 1994. 32:1-64, 1994.

Brink, K.H. and T.J. Cowles, The Coastal Transition Program. J. Geophys. Res. 96:14,637-14,647, 1991.

Brink, K.H., R.C. Beardsley, P.P. Niiler, M. Abbott, A. Huyer, S. Ramp, T. Stanton and D. Stuart, Statistical Properties of Near-Surface Flow in the California Coastal Transition Zone. J. Geophys. Res. 96:14,693-14,706, 1991.

Chelton, D.B., Seasonal variability of alongshore geostrophic velocity off central California, J. Geophys. Res., 89, 3473-3486, 1984.

Chelton, D.B., R.L. Bernstein, A. Bratkovich, and P.M. Kosro, The central California coastal circulation study, EOS Trans. AGU, 68(1), 12-13, 1987.

Chelton, D.B., A.W. Bratkovich, R.L. Bernstein, and P.M. Kosro, Poleward flow off central California during the Spring and Summer of 1981 and 1984, J. Geophys. Res., 93, 10604-10620, 1988.

Clarke, A.J., Theoretical understanding of eastern ocean boundary poleward undercurrents, in Poleward Flows Along Eastern Oceanic Boundaries, Coastal Estuarine Stud., no. 34, pp. 26-39, Springer-Verlag, New York, 1989.

Collins, C.A., R.G. Paquette, and S.R. Ramp, Annual variability of ocean currents at 350-m depth over the continental slope of Point Sur, California, Calif. Coop. Oceanic Fish. Invest. Rep., 37, 257-263, 1996.

Cushing, D.H., Upwelling and fish production. FAO Fish. Tech. Pap. 84. 40 pp, 1969.

Denbo, D.W., K. Polzin, J.S. Allen, A. Huyer, and R.L. Smith, Current meter observations over the continental shelf off Oregon and California, February 1981 - January 1984, Data Rpt 112, Oregon State University, 7 chapters + appendix, 1984.

Dorman, C.E and C.D. Winant, Buoy observations of the atmosphere along the west coast of the United States, 1981-1990. J. Geophys Res., 100:16,029-16,044, 1995.

Ekman, V.W., On the influence of the earth's rotation on ocean currents, Arkiv for Matematik, Astronomi, och Fysik, 2, 1-52, 1905.

Flament, P., A note on seawater spiciness and diffusive stability, unpublished, 1986.

Gezgin, E., A study on hydrographic conditions and salt budget calculation for the Gulf of the Farallones with the data collected in August 1990, M.S. Thesis, Naval Postgraduate School, Monterey, CA, 82 pp., 1991.

Graham, W.M., J.G. Field and D.C. Potts, Persistent "upwelling shadows" and their influence on Zooplankton distribution. Marine Biology. 114:561-570, 1992.

Hickey, B.M., The California current system - hypotheses and facts, Prog. Oceanog., 8, 191-279, 1979.

Hickey, B.M., Alongshore coherence on the Pacific Northwest continental shelf, J. Phys. Oceanog., 11, 822-835, 1981.

Hickey, B.M., Western North America, Tip of Baja to Vancouver Island, from Liege Mtg, to be included in "The Sea", 1996.

Huyer, A. and P.M. Kosro, Mesoscale surveys over the slope and shelf in the upwelling region near Point Arena, California, J. Geophys. Res., 92, 1655-1682, 1987.

Huyer, A., E.J.C. Sobey and R.L. Smith, The spring transition in currents over the Oregon continental Shelf. J. Geophys. Res. 84:6,995-7,011, 1979.

Huyer, A., Coastal upwelling in the California Current System. Progress in Oceanography, 12, 259-284, 1983.

Huyer, A., P.M. Kosro, S.J. Lentz, and R.C. Beardsley, Poleward flow in the California Current system, in Poleward Flows Along Eastern Oceanic Boundaries, Coastal Estuarine Stud., no. 34, pp. 142-156, Springer-Verlag, New York, 1989.

Johnson, J.E., An assessment of data requirements for quasi-geostrophic nowcasts and hindcasts of a mesoscale eddy field in the California Current System with application to the Fall Transition, Ph.D. Dissertation, Naval Postgraduate School, Monterey, CA, 345 pp., 1990.

Kelly, K.A., The influence of wind and topography on the sea surface temperature patterns over the northern California slope. J. Geophys. Res., 90(C6):11,783-11,798, 1985.

Kosro, P. M., A. Huyer, A. S Ramp, R.L. Smith, F. P. Chavez, T. J. Cowles, M. R. Abbott, P. T. Strub, R. T. Barber,, P. F. Jessen and L. F. Small, The structure of the Transition Zone between coastal waters and the open ocean off northern California, winter and spring 1987. J. Geophys. Res. 92:1,637-1,654, 1987.

Largier, J. L., Hydrodynamic exchange between San Francisco Bay and the ocean: the role of ocean circulation and stratification, pages 69-104 in San Francisco Bay: the Ecosystem, ed. J.T. Hollinbaugh, American Assoc. for the Advancement of Sci., San Francisco, CA, 1996.

Lentz, S.J., A description of the 1981 and 1982 spring transitions over the northern California shelf. J. Geophys. Res. 92:1,545-1,567, 1987.

Lynn, R.J., Seasonal variation of temperature and salinity at 10 m in the California Current, California, Calif. Coop. Oceanic Fish. Invest. Rep., 11, 157-186, 1967.

Lynn, R.J., K.A. Bliss, and L.E. Eber, Vertical and horizontal distributions of seasonal mean temperature, salinity, sigma-t, stability, dynamic height, oxygen and oxygen saturation in the California Current, 1950-1978, CalCOFI Atlas 30, 513 pp., State of Calif. Mar. Res. Comm., La Jolla, 1982.
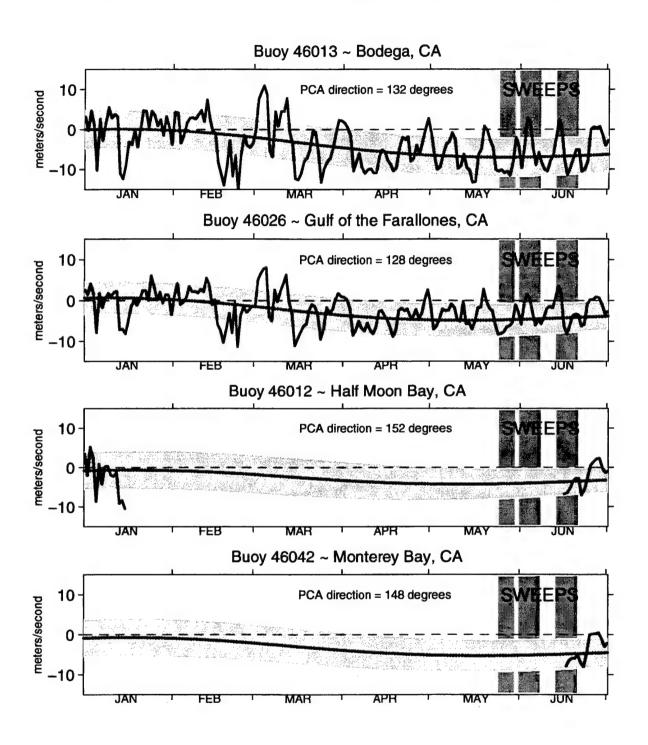
Lynn, R.J. and J.J. Simpson, The California Current system: the seasonal variability of its physical characteristics, J. Geophys. Res., 92, 12,947-12,966, 1987.

Lynn, R.J., F.B. Schwing, and T.L. Hayward, The effect of the 1991-1993 ENSO on the California Current system, Calif. Coop. Oceanic Fish. Invest. Rep., 36, 57-71, 1995.

McCreary, J.P., P.K. Kundu, and S.Y. Chao, On the dynamics of the California Current system, J. Mar. Res., 45, 1-32, 1987.

Morgan, P.P., SEAWATER: a library of MATLAB computational routines for the properties of sea water, CSIRO Marine Lab. Rep. 222, Tasmania, Australia, 1994.

Nelson, C.S., Wind stress and wind stress curl over the California current, U.S. Dept. Of Commer., NOAA Tech. Rep. NMFS-SSRF-714, 89 pp., 1977.

Parker, H.A., Variations in coastal circulation off central California, spring-summer of 1993, 1994, 1995, M.S. Thesis, Naval Postgraduate School, Monterey, CA, 1996.

Pavlova, Y.V., Seasonal variations of the California Current, Oceanology, 6, 806-814, 1966.

Petzrick, E.P., C.A. Collins, and W.C. Boicourt, Currents through the Golden Gate, pages 105-122 in San Francisco Bay: the Ecosystem, ed. J.T. Hollinbaugh, American Assoc. for the Advancement of Sci., San Francisco, CA, 1996.

Pickard, G.L., Descriptive Physical Oceanography, 214 pp., Pergamon, New York, 1964.

Pond, S. and G.L. Pickard, Introductory Dynamical Oceanography, 2nd ed., Pergamon Press, Oxford, 329 pp., 1983.

Ramp, S.R., P.F. Jessen, K.H. Brink, P.P. Niiler, F.L. Daggett and J.S. Best, The physical structure of cold filaments near Point Arena, California, during June 1987. J. Geophys. Res. 96:14,859-14,883, 1991.

Ramp S.R. and C.L. Abbott, The vertical structure of currents over the continental shelf off Point Sur, CA during spring 1990. Unpublished, 1992.

Ramp, S.R., N. Garfield, C.A. Collins, L.K. Rosenfeld, and F. Schwing, Circulation studies over the continental shelf and slope near the Farallon Islands, CA, Naval Postgraduate School Technical Report NPS-OC-95-004, Monterey, CA, 1995.
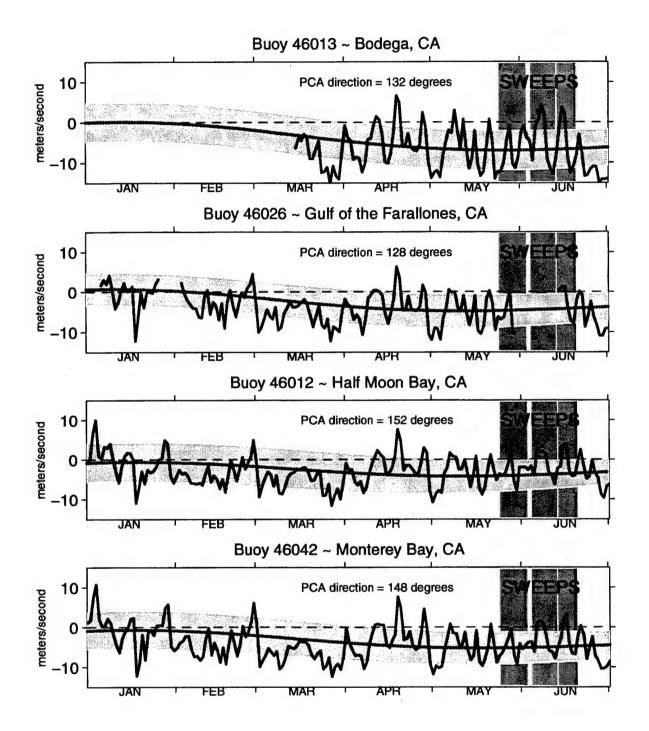
Ramp, S.R., J.L. McClean, C.A. Collins, A.J. Semtner, and K.A.S. Hays, Observations and modeling of the 1991-1992 El Niño signal off central California, J. Geophys. Res., 102, 5553-5582, 22 pp., 1997.

Reid, J.L. Jr., G.I. Roden, and J.G. Wyllie, Studies of the California Current System, California, Calif. Coop. Oceanic Fish. Invest. Rep., 6, 27-56, 1958.

Reid, J.L. Jr. and A. W. Mantyla, The effects of the geostrophic flow upon coastal sea elevations in the northen Pacific Ocean, J. Geophys. Res., 81, 3100-3110, 1976.

Rosenfeld, L.K., F.B. Schwing, N. Garfield, and D.E. Tracy, Bifurcated flow from an upwelling center: a cold source for Monterey Bay, Cont. Shelf Res., 14, 931-964, 1994.

Roughgarden et al;, Collisions of upwelling fronts with the intertidal zone; the cause of recruitment pulses in barnacle populations of central California. Acta Ecologica, 12:35-51, 1991.

Ryther, J.H., Photosynthesis and fish production in the sea. Science 166:72-76, 1969.

Sakuma, K.M., F.B. Schwing, K. Baltz, D. Roberts, H.A. Parker, and S. Ralston, The physical oceanography off the central California coast during May-June 1995: a summary of CTD data from pelagic juvenile rockfish surveys, NOAA Tech. Rep. NOAA-TM-NMFS-231, US Dept of Commer., 144 pp., 1996.

Schwing, F.B., D.M. Husby, N. Garfield, and D.E. Tracy, Mesoscale oceanic response to wind events off central California in Spring 1989: CTD surveys and AVHRR imagery, CalCOFI Reports, 32, 47-62, 1991.

Schwing, F.B., M. O'Farrell, J. Steger, and K. Baltz, Coastal upwelling indices, west coast of North America 1946-1995, NOAA Tech. Rep. NOAA-TM-NMFS-SWFSC-231, US Dept of Commer., 207 pp., 1996.

Schwing, F.B., T.L. Hayward, T. Murphree, K.M. Sakuma, A.S. Mascarenas, A.W. Mantyla, S.I.L. Castillo, S.L. Cummings, K. Baltz and D.G. Ainley, The state of the California Current, 1996-1997: mixed signals from the tropics, California, Calif. Coop. Oceanic Fish. Invest. Rep., 1997 (in press).

Send, U., R.C. Beardsley, and C.D. Winant, Relaxation from upwelling in the Coastal Ocean Dynamics Experiment, J. Geophys. Res., 92:1,683-1,698, 1987.

Simpson, J.J., El Nino-induced onshore transport in the California Current during 1982-1983. Geophys. Res. Lett., Vol. 11, 3, 233-236, 1984.
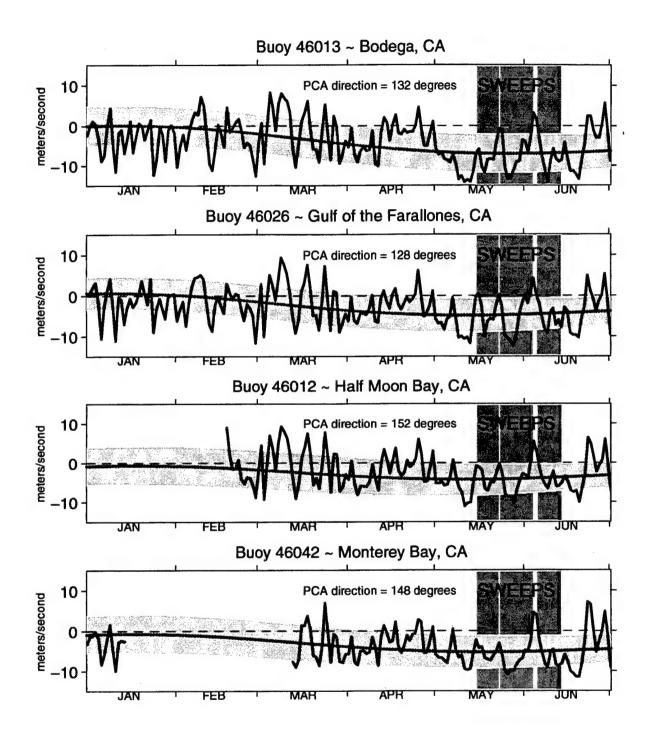
Smith, R.L., Upwelling. Oceanog. Mar. Biol. Ann Rev., 6:11-46, 1968.

Smith, R.L., The physical processes of coastal ocean upwelling systems. Dahlem Workshop on Upwelling in the Ocean: Modern Processes and Ancient Records, 1994.

Steger, J., Use of Ship-mounted acoustic doppler current profiler data to study mesoscale oceanic circulation patterns in the Archipelago de Colon (Galapagos Islands) and the Gulf of the Farallones. Ph.D. Dissertation, Naval Postgraduate School, Monterey, CA, 1997.

Storch, H.von and Navarra, A. (Eds.), Analysis of Climate Variability: Applications of Statistical Techniques. Springer-Verlag Berlin Heidelberg New York, 1995.

Strub, P.T., J.S. Allen, A. Huyer, and R.L. Smith, Seasonal cycles of currents, temperatures, winds, and sea level over the northeast Pacific continental shelf: 35°N to 48°N, J. Geophys. Res., 92, 1507-1526, 1987.

Strub, P.T., and the CTZ Group, The nature of cold filaments in the California Current System. J. Geophys. Res. 92:1,527-1,544, 1991.

Sverdrup, H.U., M.W. Johnson, and R.H. Fleming, The Oceans, Their Physics, Chemistry, and General Biology, 1087pp., Prentice-Hall, Englewood Cliffs, N.J., 1942.

Tisch, T.D., S.R. Ramp, and C.A. Collins, Observations of the geostrophic current and water mass characteristics off Point Sur, California, from May 1988 through November 1989, J. Geophys. Res., 97, 12,535-12,555, 1992.

Wickham, J.B., A.A. Bird, and C.N.K. Mooers, Mean and variable flow over the central California continental margin, 1978-1980, Cont. Shelf Res., 7, 827-849, 1987.

Winant, C.D., R.C. Beardsley, and R.E. Davis, Moored wind, temperature, and current observations made during Coastal Ocean Dynamics Experiments 1 and 2 over the northern California continental shelf and upper slope, J. Geophys. Res., 92, 1569-1604, 1987.

Wyllie, J.G., Geostrophic flow of the California Current at the surface and at 200 m, CalCOFI Atlas 4, 303 pp., State of Calif. Mar. Res. Comm., La Jolla, 1966.
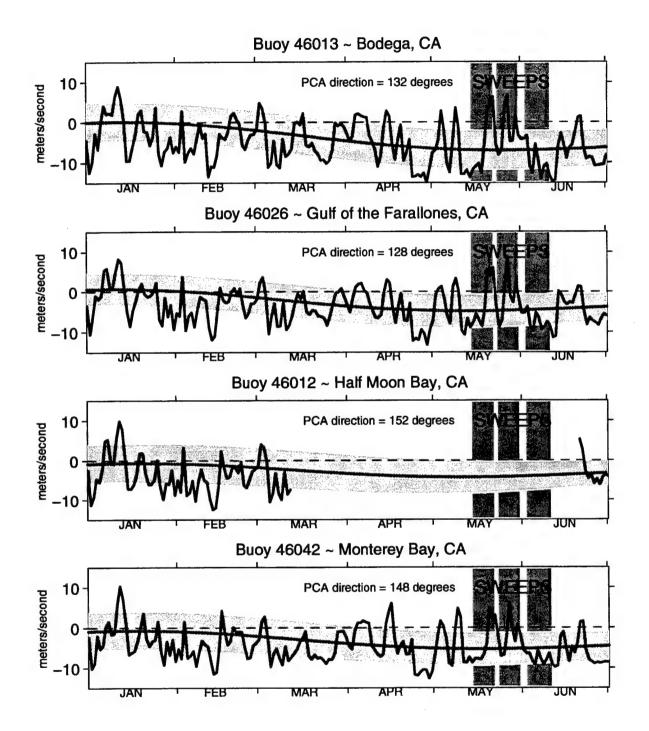
APPENDIX A. TIME SERIES PLOTS OF SURFACE CONDITIONS, 1987-1996
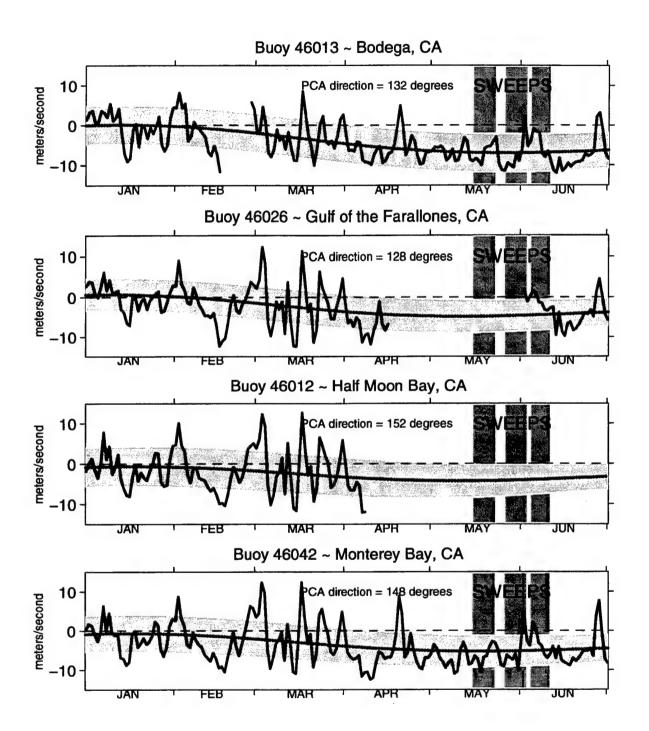
The data shown in this appendix are daily values of NOAA buoy alongshore wind, buoy sea surface temperature, Southeast Farallon Island sea surface temperature, and SEFI sea surface salinity during the first six months of each year from 1987-1996. The daily values are plotted on a climatology background where the smooth bold line represents the least squares regression fit of the daily data to a biharmonic signal. The light gray shaded envelope about the daily fits line is plus and minus one standard error. The dark gray shaded area represents the typical cruise period for the annual NMFS juvenile rockfish survey aboard the *NOAA Ship David Starr Jordan.*

Alongshore Winds from NOAA NDBC Buoys ~ 1987

Buoy 46013 ~ Bodega, CA

PCA direction = 132 degrees

SWEEPS

Buoy 46026 ~ Gulf of the Farallones, CA

PCA direction = 128 degrees

SWEEPS

Buoy 46012 ~ Half Moon Bay, CA

PCA direction = 152 degrees

SWEEPS

Buoy 46042 ~ Monterey Bay, CA

PCA direction = 148 degrees

SWEEPS

Alongshore Winds from NOAA NDBC Buoys ~ 1988

Buoy 46013 ~ Bodega, CA

PCA direction = 132 degrees

Buoy 46026 ~ Gulf of the Farallones, CA

PCA direction = 128 degrees

Buoy 46012 ~ Half Moon Bay, CA

PCA direction = 152 degrees

Buoy 46042 ~ Monterey Bay, CA

PCA direction = 148 degrees

Alongshore Winds from NOAA NDBC Buoys ~ 1989

Buoy 46013 ~ Bodega, CA

PCA direction = 132 degrees

Buoy 46026 ~ Gulf of the Farallones, CA

PCA direction = 128 degrees

Buoy 46012 ~ Half Moon Bay, CA

PCA direction = 152 degrees

Buoy 46042 ~ Monterey Bay, CA

PCA direction = 148 degrees

114

Alongshore Winds from NOAA NDBC Buoys ~ 1990

Buoy 46013 ~ Bodega, CA

PCA direction = 132 degrees

Buoy 46026 ~ Gulf of the Farallones, CA

PCA direction = 128 degrees

Buoy 46012 ~ Half Moon Bay, CA

PCA direction = 152 degrees

Buoy 46042 ~ Monterey Bay, CA

PCA direction = 148 degrees

115

Alongshore Winds from NOAA NDBC Buoys ~ 1991

Buoy 46013 ~ Bodega, CA

PCA direction = 132 degrees

Buoy 46026 ~ Gulf of the Farallones, CA

PCA direction = 128 degrees

Buoy 46012 ~ Half Moon Bay, CA

PCA direction = 152 degrees

Buoy 46042 ~ Monterey Bay, CA

PCA direction = 148 degrees

Alongshore Winds from NOAA NDBC Buoys ~ 1992

Buoy 46013 ~ Bodega, CA

PCA direction = 132 degrees

SWEEPS

Buoy 46026 ~ Gulf of the Farallones, CA

PCA direction = 128 degrees

SWEEPS

Buoy 46012 ~ Half Moon Bay, CA

PCA direction = 152 degrees

SWEEPS

Buoy 46042 ~ Monterey Bay, CA

PCA direction = 148 degrees

SWEEPS

Alongshore Winds from NOAA NDBC Buoys ~ 1993

Buoy 46013 ~ Bodega, CA

PCA direction = 132 degrees

Buoy 46026 ~ Gulf of the Farallones, CA

PCA direction = 128 degrees

Buoy 46012 ~ Half Moon Bay, CA

PCA direction = 152 degrees

Buoy 46042 ~ Monterey Bay, CA

PCA direction = 148 degrees

118

Alongshore Winds from NOAA NDBC Buoys ~ 1994

Buoy 46013 ~ Bodega, CA

PCA direction = 132 degrees

Buoy 46026 ~ Gulf of the Farallones, CA

PCA direction = 128 degrees

Buoy 46012 ~ Half Moon Bay, CA

PCA direction = 152 degrees

Buoy 46042 ~ Monterey Bay, CA

PCA direction = 148 degrees

119

Alongshore Winds from NOAA NDBC Buoys ~ 1995

Buoy 46013 ~ Bodega, CA

PCA direction = 132 degrees

SWEEPS

Buoy 46026 ~ Gulf of the Farallones, CA

PCA direction = 128 degrees

SWEEPS

Buoy 46012 ~ Half Moon Bay, CA

PCA direction = 152 degrees

SWEEPS

Buoy 46042 ~ Monterey Bay, CA

PCA direction = 148 degrees

SWEEPS

Alongshore Winds from NOAA NDBC Buoys ~ 1996

Buoy 46013 ~ Bodega, CA

PCA direction = 132 degrees

Buoy 46026 ~ Gulf of the Farallones, CA

PCA direction = 128 degrees

Buoy 46012 ~ Half Moon Bay, CA

PCA direction = 152 degrees

Buoy 46042 ~ Monterey Bay, CA

PCA direction = 148 degrees

Sea Surface Temperatures from NOAA NDBC Buoys ~ 1987

Buoy 46013 ~ Bodega, CA

Buoy 46026 ~ Gulf of the Farallones, CA

Buoy 46012 ~ Half Moon Bay, CA

Buoy 46042 ~ Monterey Bay, CA

Sea Surface Temperatures from NOAA NDBC Buoys ~ 1988

Buoy 46013 ~ Bodega, CA

Buoy 46026 ~ Gulf of the Farallones, CA

Buoy 46012 ~ Half Moon Bay, CA

Buoy 46042 ~ Monterey Bay, CA

Sea Surface Temperatures from NOAA NDBC Buoys ~ 1989

Buoy 46013 ~ Bodega, CA

Buoy 46026 ~ Gulf of the Farallones, CA

Buoy 46012 ~ Half Moon Bay, CA

Buoy 46042 ~ Monterey Bay, CA

Sea Surface Temperatures from NOAA NDBC Buoys ~ 1990

Buoy 46013 ~ Bodega, CA

Buoy 46026 ~ Gulf of the Farallones, CA

Buoy 46012 ~ Half Moon Bay, CA

Buoy 46042 ~ Monterey Bay, CA

Sea Surface Temperatures from NOAA NDBC Buoys ~ 1991

Buoy 46013 ~ Bodega, CA

Buoy 46026 ~ Gulf of the Farallones, CA

Buoy 46012 ~ Half Moon Bay, CA

Buoy 46042 ~ Monterey Bay, CA

126

Sea Surface Temperatures from NOAA NDBC Buoys ~ 1992

Buoy 46013 ~ Bodega, CA

Buoy 46026 ~ Gulf of the Farallones, CA

Buoy 46012 ~ Half Moon Bay, CA

Buoy 46042 ~ Monterey Bay, CA

127

Sea Surface Temperatures from NOAA NDBC Buoys ~ 1993

Buoy 46013 ~ Bodega, CA

Buoy 46026 ~ Gulf of the Farallones, CA

Buoy 46012 ~ Half Moon Bay, CA

Buoy 46042 ~ Monterey Bay, CA

Sea Surface Temperatures from NOAA NDBC Buoys ~ 1994

Buoy 46013 ~ Bodega, CA

Buoy 46026 ~ Gulf of the Farallones, CA

Buoy 46012 ~ Half Moon Bay, CA

Buoy 46042 ~ Monterey Bay, CA

Sea Surface Temperatures from NOAA NDBC Buoys ~ 1995

Buoy 46013 ~ Bodega, CA

Buoy 46026 ~ Gulf of the Farallones, CA

Buoy 46012 ~ Half Moon Bay, CA

Buoy 46042 ~ Monterey Bay, CA

130

Sea Surface Temperatures from NOAA NDBC Buoys ~ 1996

Buoy 46013 ~ Bodega, CA

Buoy 46026 ~ Gulf of the Farallones, CA

Buoy 46012 ~ Half Moon Bay, CA

Buoy 46042 ~ Monterey Bay, CA

131

Temperature and Salinity at Southeast Farallon Island

Sea Surface Temperature ~ 1987

Surface Salinity ~ 1987

Sea Surface Temperature ~ 1988

Surface Salinity ~ 1988

Temperature and Salinity at Southeast Farallon Island

Sea Surface Temperature ~ 1989

Surface Salinity ~ 1989

Sea Surface Temperature ~ 1990

Surface Salinity ~ 1990

133

Temperature and Salinity at Southeast Farallon Island

Sea Surface Temperature ~ 1991

Surface Salinity ~ 1991

Sea Surface Temperature ~ 1992

Surface Salinity ~ 1992

Temperature and Salinity at Southeast Farallon Island

Sea Surface Temperature ~ 1993

Surface Salinity ~ 1993

Sea Surface Temperature ~ 1994

Surface Salinity ~ 1994

Temperature and Salinity at Southeast Farallon Island

Sea Surface Temperature ~ 1995

Surface Salinity ~ 1995

Sea Surface Temperature ~ 1996

Surface Salinity ~ 1996

APPENDIX B. CONTOUR CHARTS OF CTD VARIABLES FROM ALL SURVEY SWEEPS, 1987-1996

The following charts are contour plots of subsurface oceanographic conditions based on CTD measurements taken during each sweep of the annual NMFS juvenile rockfish surveys. The CTD variables appearing in the contour charts are:
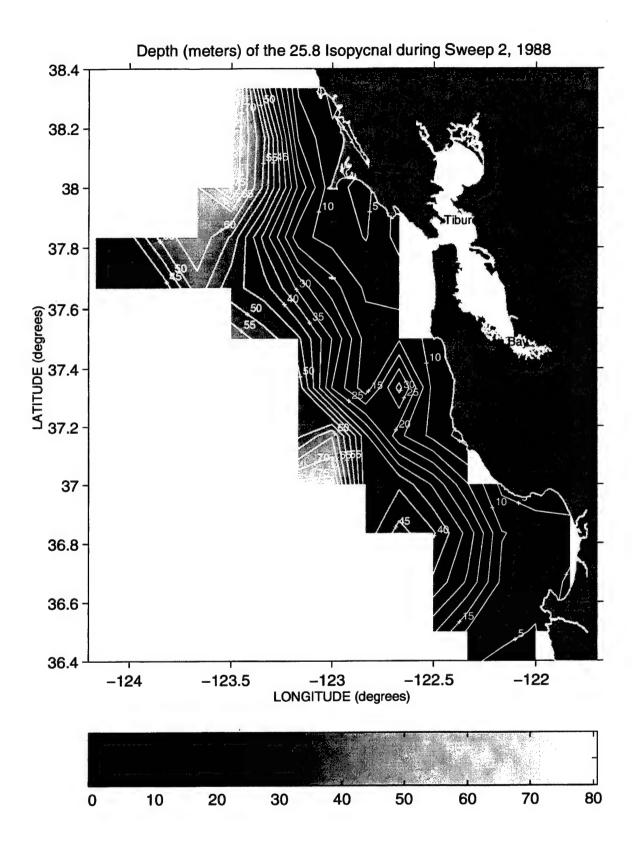
* **Depth of the 25.8 kg/m^3 isopycnal**

* **Depth of the 26.2 kg/m^3 isopycnal**

* **Thickness between the 25.8 kg/m^3 and 26.2 kg/m^3 isopycnals**

* **Salinity on the 25.8 kg/m^3 isopycnal**

* **Salinity on the 26.2 kg/m^3 isopycnal**

* **Mixed layer depth**

Depth (meters) of the 25.8 Isopycnal during Sweep 1, 1987

138

Depth (meters) of the 25.8 Isopycnal during Sweep 2, 1987

Depth (meters) of the 25.8 Isopycnal during Sweep 3, 1987

Depth (meters) of the 25.8 Isopycnal during Sweep 1, 1988

Depth (meters) of the 25.8 Isopycnal during Sweep 2, 1988

142

Depth (meters) of the 25.8 Isopycnal during Sweep 3, 1988

Depth (meters) of the 25.8 Isopycnal during Sweep 1, 1989

Depth (meters) of the 25.8 Isopycnal during Sweep 2, 1989

Depth (meters) of the 25.8 Isopycnal during Sweep 3, 1989

Depth (meters) of the 25.8 Isopycnal during Sweep 1, 1990

Depth (meters) of the 25.8 Isopycnal during Sweep 2, 1990

148

Depth (meters) of the 25.8 Isopycnal during Sweep 3, 1990

Depth (meters) of the 25.8 Isopycnal during Sweep 1, 1991

Depth (meters) of the 25.8 Isopycnal during Sweep 2, 1991

Depth (meters) of the 25.8 Isopycnal during Sweep 3, 1991

Depth (meters) of the 25.8 Isopycnal during Sweep 1, 1992

153

Depth (meters) of the 25.8 Isopycnal during Sweep 2, 1992

Depth (meters) of the 25.8 Isopycnal during Sweep 3, 1992

Depth (meters) of the 25.8 Isopycnal during Sweep 1, 1993

Depth (meters) of the 25.8 Isopycnal during Sweep 2, 1993

Depth (meters) of the 25.8 Isopycnal during Sweep 3, 1993

Depth (meters) of the 25.8 Isopycnal during Sweep 1, 1994

Depth (meters) of the 25.8 Isopycnal during Sweep 2, 1994

Depth (meters) of the 25.8 Isopycnal during Sweep 3, 1994

Depth (meters) of the 25.8 Isopycnal during Sweep 1, 1995

Depth (meters) of the 25.8 Isopycnal during Sweep 2, 1995

Depth (meters) of the 25.8 Isopycnal during Sweep 3, 1995

Depth (meters) of the 25.8 Isopycnal during Sweep 1, 1996

Depth (meters) of the 25.8 Isopycnal during Sweep 2, 1996

Depth (meters) of the 25.8 Isopycnal during Sweep 3, 1996

Depth (meters) of the 26.2 Isopycnal during Sweep 1, 1987

Depth (meters) of the 26.2 Isopycnal during Sweep 2, 1987

Depth (meters) of the 26.2 Isopycnal during Sweep 3, 1987

Depth (meters) of the 26.2 Isopycnal during Sweep 1, 1988

Depth (meters) of the 26.2 Isopycnal during Sweep 2, 1988

172

Depth (meters) of the 26.2 Isopycnal during Sweep 3, 1988

Depth (meters) of the 26.2 Isopycnal during Sweep 1, 1989

174

Depth (meters) of the 26.2 Isopycnal during Sweep 2, 1989

Depth (meters) of the 26.2 Isopycnal during Sweep 3, 1989

Depth (meters) of the 26.2 Isopycnal during Sweep 1, 1990

Depth (meters) of the 26.2 Isopycnal during Sweep 2, 1990

Depth (meters) of the 26.2 Isopycnal during Sweep 3, 1990

Depth (meters) of the 26.2 Isopycnal during Sweep 1, 1991

Depth (meters) of the 26.2 Isopycnal during Sweep 2, 1991

Depth (meters) of the 26.2 Isopycnal during Sweep 3, 1991

Depth (meters) of the 26.2 Isopycnal during Sweep 1, 1992

Depth (meters) of the 26.2 Isopycnal during Sweep 2, 1992

Depth (meters) of the 26.2 Isopycnal during Sweep 3, 1992

Depth (meters) of the 26.2 Isopycnal during Sweep 1, 1993

Depth (meters) of the 26.2 Isopycnal during Sweep 2, 1993

Depth (meters) of the 26.2 Isopycnal during Sweep 3, 1993

Depth (meters) of the 26.2 Isopycnal during Sweep 1, 1994

Depth (meters) of the 26.2 Isopycnal during Sweep 2, 1994

Depth (meters) of the 26.2 Isopycnal during Sweep 3, 1994

Depth (meters) of the 26.2 Isopycnal during Sweep 1, 1995

Depth (meters) of the 26.2 Isopycnal during Sweep 2, 1995

193

Depth (meters) of the 26.2 Isopycnal during Sweep 3, 1995

Depth (meters) of the 26.2 Isopycnal during Sweep 1, 1996

Depth (meters) of the 26.2 Isopycnal during Sweep 2, 1996

Depth (meters) of the 26.2 Isopycnal during Sweep 3, 1996

Thickness(meters) between the 25.8 and 26.2 isopycnals ~ Sweep 1, 1987

Thickness(meters) between the 25.8 and 26.2 isopycnals ~ Sweep 2, 1987

Thickness(meters) between the 25.8 and 26.2 isopycnals ~ Sweep 3, 1987

Thickness(meters) between the 25.8 and 26.2 isopycnals ~ Sweep 1, 1988

Thickness(meters) between the 25.8 and 26.2 isopycnals ~ Sweep 2, 1988

Thickness(meters) between the 25.8 and 26.2 isopycnals ~ Sweep 3, 1988

Thickness(meters) between the 25.8 and 26.2 isopycnals ~ Sweep 1, 1989

Thickness(meters) between the 25.8 and 26.2 isopycnals ~ Sweep 2, 1989

Thickness(meters) between the 25.8 and 26.2 isopycnals ~ Sweep 3, 1989

Thickness(meters) between the 25.8 and 26.2 isopycnals ~ Sweep 1, 1990

Thickness(meters) between the 25.8 and 26.2 isopycnals ~ Sweep 2, 1990

Thickness(meters) between the 25.8 and 26.2 isopycnals ~ Sweep 3, 1990

209

Thickness(meters) between the 25.8 and 26.2 isopycnals ~ Sweep 1, 1991

Thickness(meters) between the 25.8 and 26.2 isopycnals ~ Sweep 2, 1991

Thickness(meters) between the 25.8 and 26.2 isopycnals ~ Sweep 3, 1991

Thickness(meters) between the 25.8 and 26.2 isopycnals ~ Sweep 1, 1992

Thickness(meters) between the 25.8 and 26.2 isopycnals ~ Sweep 2, 1992

Thickness(meters) between the 25.8 and 26.2 isopycnals ~ Sweep 3, 1992

Thickness(meters) between the 25.8 and 26.2 isopycnals ~ Sweep 1, 1993

Thickness(meters) between the 25.8 and 26.2 isopycnals ~ Sweep 2, 1993

Thickness(meters) between the 25.8 and 26.2 isopycnals ~ Sweep 3, 1993

Thickness(meters) between the 25.8 and 26.2 isopycnals ~ Sweep 1, 1994

Thickness(meters) between the 25.8 and 26.2 isopycnals ~ Sweep 2, 1994

Thickness(meters) between the 25.8 and 26.2 isopycnals ~ Sweep 3, 1994

Thickness(meters) between the 25.8 and 26.2 isopycnals ~ Sweep 1, 1995

Thickness(meters) between the 25.8 and 26.2 isopycnals ~ Sweep 2, 1995

Thickness(meters) between the 25.8 and 26.2 isopycnals ~ Sweep 3, 1995

Thickness(meters) between the 25.8 and 26.2 isopycnals ~ Sweep 1, 1996

Thickness(meters) between the 25.8 and 26.2 isopycnals ~ Sweep 2, 1996

Thickness(meters) between the 25.8 and 26.2 isopycnals ~ Sweep 3, 1996

Salinity (PSS) at the 25.8 Isopycnal during Sweep 1, 1987

Salinity (PSS) at the 25.8 Isopycnal during Sweep 2, 1987

Salinity (PSS) at the 25.8 Isopycnal during Sweep 3, 1987

Salinity (PSS) at the 25.8 Isopycnal during Sweep 1, 1988

231

Salinity (PSS) at the 25.8 Isopycnal during Sweep 2, 1988

Salinity (PSS) at the 25.8 Isopycnal during Sweep 3, 1988

Salinity (PSS) at the 25.8 Isopycnal during Sweep 1, 1989

Salinity (PSS) at the 25.8 Isopycnal during Sweep 2, 1989

Salinity (PSS) at the 25.8 Isopycnal during Sweep 3, 1989

Salinity (PSS) at the 25.8 Isopycnal during Sweep 1, 1990

Salinity (PSS) at the 25.8 Isopycnal during Sweep 2, 1990

238

Salinity (PSS) at the 25.8 Isopycnal during Sweep 3, 1990

Salinity (PSS) at the 25.8 Isopycnal during Sweep 1, 1991

Salinity (PSS) at the 25.8 Isopycnal during Sweep 2, 1991

Salinity (PSS) at the 25.8 Isopycnal during Sweep 3, 1991

Salinity (PSS) at the 25.8 Isopycnal during Sweep 1, 1992

243

Salinity (PSS) at the 25.8 Isopycnal during Sweep 2, 1992

Salinity (PSS) at the 25.8 Isopycnal during Sweep 3, 1992

Salinity (PSS) at the 25.8 Isopycnal during Sweep 1, 1993

Salinity (PSS) at the 25.8 Isopycnal during Sweep 2, 1993

Salinity (PSS) at the 25.8 Isopycnal during Sweep 3, 1993

Salinity (PSS) at the 25.8 Isopycnal during Sweep 1, 1994

Salinity (PSS) at the 25.8 Isopycnal during Sweep 2, 1994

Salinity (PSS) at the 25.8 Isopycnal during Sweep 3, 1994

Salinity (PSS) at the 25.8 Isopycnal during Sweep 1, 1995

Salinity (PSS) at the 25.8 Isopycnal during Sweep 2, 1995

Salinity (PSS) at the 25.8 Isopycnal during Sweep 3, 1995

Salinity (PSS) at the 25.8 Isopycnal during Sweep 1, 1996

Salinity (PSS) at the 25.8 Isopycnal during Sweep 2, 1996

Salinity (PSS) at the 25.8 Isopycnal during Sweep 3, 1996

Salinity (PSS) at the 26.2 Isopycnal during Sweep 1, 1987

Salinity (PSS) at the 26.2 Isopycnal during Sweep 2, 1987

Salinity (PSS) at the 26.2 Isopycnal during Sweep 3, 1987

Salinity (PSS) at the 26.2 Isopycnal during Sweep 1, 1988

Salinity (PSS) at the 26.2 Isopycnal during Sweep 2, 1988

Salinity (PSS) at the 26.2 Isopycnal during Sweep 3, 1988

Salinity (PSS) at the 26.2 Isopycnal during Sweep 1, 1989

Salinity (PSS) at the 26.2 Isopycnal during Sweep 2, 1989

Salinity (PSS) at the 26.2 Isopycnal during Sweep 3, 1989

Salinity (PSS) at the 26.2 Isopycnal during Sweep 1, 1990

Salinity (PSS) at the 26.2 Isopycnal during Sweep 2, 1990

Salinity (PSS) at the 26.2 Isopycnal during Sweep 3, 1990

Salinity (PSS) at the 26.2 Isopycnal during Sweep 1, 1991

Salinity (PSS) at the 26.2 Isopycnal during Sweep 2, 1991

Salinity (PSS) at the 26.2 Isopycnal during Sweep 3, 1991

Salinity (PSS) at the 26.2 Isopycnal during Sweep 1, 1992

Salinity (PSS) at the 26.2 Isopycnal during Sweep 2, 1992

Salinity (PSS) at the 26.2 Isopycnal during Sweep 3, 1992

Salinity (PSS) at the 26.2 Isopycnal during Sweep 1, 1993

Salinity (PSS) at the 26.2 Isopycnal during Sweep 2, 1993

Salinity (PSS) at the 26.2 Isopycnal during Sweep 3, 1993

Salinity (PSS) at the 26.2 Isopycnal during Sweep 1, 1994

Salinity (PSS) at the 26.2 Isopycnal during Sweep 2, 1994

Salinity (PSS) at the 26.2 Isopycnal during Sweep 3, 1994

Salinity (PSS) at the 26.2 Isopycnal during Sweep 1, 1995

Salinity (PSS) at the 26.2 Isopycnal during Sweep 2, 1995

Salinity (PSS) at the 26.2 Isopycnal during Sweep 3, 1995

Salinity (PSS) at the 26.2 Isopycnal during Sweep 1, 1996

285

Salinity (PSS) at the 26.2 Isopycnal during Sweep 2, 1996

Salinity (PSS) at the 26.2 Isopycnal during Sweep 3, 1996

Mixed Layer Depth (meters) during Sweep 1, 1987

Mixed Layer Depth (meters) during Sweep 2, 1987

Mixed Layer Depth (meters) during Sweep 3, 1987

Mixed Layer Depth (meters) during Sweep 1, 1988

Mixed Layer Depth (meters) during Sweep 2, 1988

Mixed Layer Depth (meters) during Sweep 3, 1988

Mixed Layer Depth (meters) during Sweep 1, 1989

294

Mixed Layer Depth (meters) during Sweep 2, 1989

295

Mixed Layer Depth (meters) during Sweep 3, 1989

Mixed Layer Depth (meters) during Sweep 1, 1990

Mixed Layer Depth (meters) during Sweep 2, 1990

Mixed Layer Depth (meters) during Sweep 3, 1990

Mixed Layer Depth (meters) during Sweep 1, 1991

300

Mixed Layer Depth (meters) during Sweep 2, 1991

301

Mixed Layer Depth (meters) during Sweep 3, 1991

302

Mixed Layer Depth (meters) during Sweep 1, 1992

Mixed Layer Depth (meters) during Sweep 2, 1992

Mixed Layer Depth (meters) during Sweep 3, 1992

Mixed Layer Depth (meters) during Sweep 1, 1993

Mixed Layer Depth (meters) during Sweep 2, 1993

Mixed Layer Depth (meters) during Sweep 3, 1993

Mixed Layer Depth (meters) during Sweep 1, 1994

309

Mixed Layer Depth (meters) during Sweep 2, 1994

310

Mixed Layer Depth (meters) during Sweep 3, 1994

Mixed Layer Depth (meters) during Sweep 1, 1995

Mixed Layer Depth (meters) during Sweep 2, 1995

313

Mixed Layer Depth (meters) during Sweep 3, 1995

314

Mixed Layer Depth (meters) during Sweep 1, 1996

315

Mixed Layer Depth (meters) during Sweep 2, 1996

316

Mixed Layer Depth (meters) during Sweep 3, 1996

INITIAL DISTRIBUTION LIST

No. Copies

1. Defense Technical Information Center 2
   8725 John J. Kingman Rd., Ste 0944
   Ft. Belvoir, VA 22060-6218

2. Dudley Knox Library...2
   Naval Postgraduate School
   411 Dyer Rd.
   Monterey, CA 93943-5101

3. Dr. Curtis A. Collins, Code OC\CO...1
   Department of Oceanography
   Naval Postgraduate School
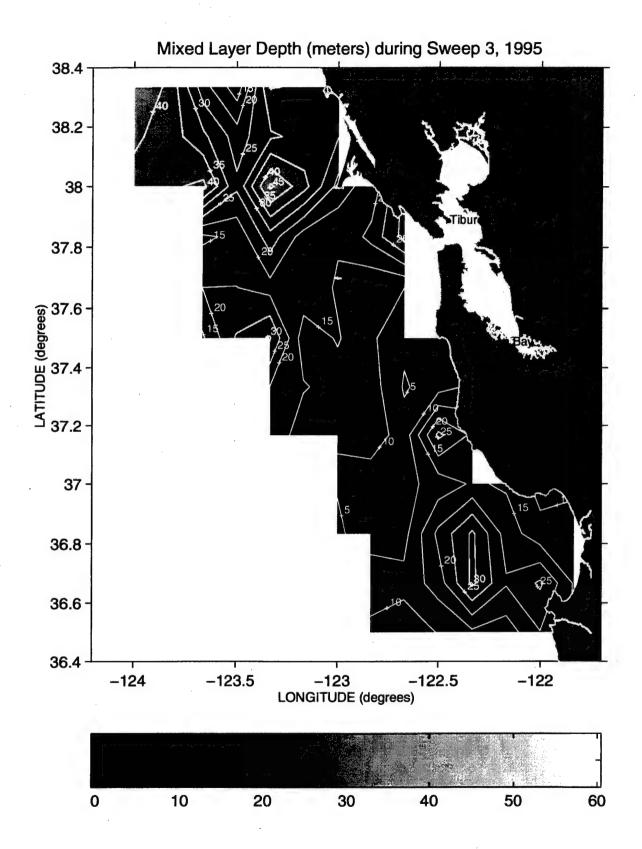   411 Dyer Rd.
   Monterey, CA 93943-5101

4. Dr. Franklin Schwing...2
   NMFS/SWFSC/PFEL
   1352 Lighthouse Ave.
   Pacific Grove, CA 93950

5. LT Kenneth Baltz...2
   NOAA Ship Chapman
   3209 Frederic Street
   Pascagoula, MS 39567

6. NOAA NMFS PFEL Library...1
   C/O Janet Mason
   1352 Lighthouse Avenue
   Pacific Grove, CA 93950

7. Dr. Leslie Rosenfeld...1
   Department of Oceanography
   Naval Postgraduate School
   411 Dyer Road
   Monterey, CA 93943-5101

8. NOAA NMFS SWFSC Library..1
   3150 Paradise Drive
   Tiburon, CA 94920

9. Groundfish Analysis Group...1
   NOAA NMFS SWFSC
   3150 Paradise Drive
   Tiburon, CA 94920

10. Carol Keiper..1
    1756 Helane Court
    Benicia, CA 94510

11. Dan Howard and Ed Ueber...1
    GOF/Cordell Bank National Marine Sanctuary
    Fort Mason Building 201
    San Francisco, CA 94123